Early induction of mouse precursor B-cell lymphomas after exposure to ionizing radiation and underlying molecular mechanisms

電離放射線被ばくによるマウス前駆 B 細胞性リンパ腫の早期発症と分子メカニズム

2022 年 1 月

千葉大学大学院融合理工学府

橘　拓孝

（千葉大学学位申請論文）

Early induction of mouse precursor B-cell lymphomas after exposure to ionizing radiation and underlying molecular mechanisms

電離放射線被ばくによるマウス前駆 B 細胞性リンパ腫の早期発症と分子メカニズム

2022 年 1 月

千葉大学大学院融合理工学府
先進理化学専攻　生物学コース

橘　拓孝

CONTENTS

GENERAL INTRODUCTION

Cancer is a disease caused by the accumulation of genetic and epigenetic changes. The genetic abnormalities include single-nucleotide variant mutations, small insertions/ deletions and chromosomal rearrangements/imbalances [1]. The epigenetic abnormalities include changes in DNA methylation, histone modifications, and non-coding RNAs [2]. These abnormalities occur in proto-oncogenes and tumor suppressor genes that control a variety of cellular process, including cell differentiation, cell cycle and apoptosis [1]. In general, dysregulation of proto-oncogenes can be caused by multiple mechanisms, such as mutational activation and over-expression through gene amplification and promoter DNA hypomethylation [1, 2]. In addition, in some leukemias and solid tumors, fusion genes, generated by chromosomal translocation, are known to act as oncogenes [3]. On the other hand, tumor suppressor genes lost their function by inactivation of both paternal and maternal alleles via genomic mutation, deletion, and promoter DNA hypermethylation [1, 2]. Occasionally, single allele inactivation of a tumor suppressor gene is sufficient to cause cancer, which is called haploinsufficiency [4]. Cancer development is a multistep process which comprises initiation, promotion and progression stages of carcinogenesis and is driven by 2 to 8 driver genes [1, 5]. For example, in human colorectal cancer, a loss-of-function mutation of the tumor suppressor gene *APC* occurs in normal epithelial cells, followed by occurrences of a gain-of-function mutation of proto-oncogene *KRAS* and deletions of tumor suppressor genes *SMAD4* and *FBXW7*, causing clonal proliferation of abnormal cells, resulting in developing benign tumor [5, 6]. Additional deletion of a tumor suppressor gene *TP53* in a cell of the clone, develops malignant tumor [5, 6].

Ionizing radiation is used in various fields including medicine, industry, and agriculture. In particular, medical use of radiation such as diagnostic imaging and cancer treatment is increasing with technological advances [7, 8]. On the other hand, exposure to ionizing radiation can potentially induce adverse health effects, including cancer and hereditary effects. These effects of ionizing radiation are caused by giving its energy to biological matter through two primary mechanisms: the direct action caused by immediate deposition of energy into DNA, and the indirect action caused by reactive oxygen species generated by deposition of energy into water [9]. Ionizing radiation induces a variety of DNA lesions, including base damage, DNA-protein cross-links, DNA single-strand breaks (SSBs), and DNA double-strand breaks (DSBs) [10-12]. Among them, DSBs are known as the primary lesions responsible for the biological effects of ionizing radiation [12]. In mammalian cells, two distinct pathways for repairing DSBs are known as homologous recombination (HR) and non-homologous end-joining (NHEJ) [13]. HR is a highly accurate repair process in which the complementary strand of the sister chromatid serves as a template and thus the use of this repair process is restricted to S to G2/M phases of the cell cycle [13, 14]. On the other hand, NHEJ occurs throughout the cell cycle and directly ligates the broken DNA ends, which is considered to be error-prone [14, 15]. Errors during DNA repair after radiation exposure can lead to the induction of genomic abnormalities and consequently to tumorigenesis.

Epidemiological studies of Japanese atomic bomb survivors have reported that ionizing radiation is a risk factor for cancer, and several organs, including skin, breast, colon, thyroid, and hematopoietic tissue, show particularly high excess cancer risks in radiation dose-dependent manners [16, 17]. In addition, these studies have shown that exposure to ionizing radiation at a younger age increases the risk of several solid cancers,

such as skin and thyroid cancers, and leukemia [16, 17]. Furthermore, a gender difference in the risk have been observed in several cancers (e.g., a higher radiation-induced risk of colorectal cancer, nervous system cancer and leukemia in men than in women) [16, 17]. In particular, there was a striking effect of radiation exposure on the development of acute lymphoblastic leukemia (ALL) during a short period after exposure [16].

ALL is a disease characterized by lack of differentiation and uncontrolled proliferation of precursor B- or T-cells, and ~80 % of which are known as precursor B-cell neoplasm [18]. Lymphoid development is a highly ordered multistep process by which mature B- and T- cells are generated from undifferentiated progenitor cells. The development of B-cells is accompanied in the marrow through the rearrangement of immunoglobulin heavy- and light-chain genes in precursor B-cells and they subsequently migrate to spleen and lymph nodes [19, 20]. On the other hand, the T-cell development is mainly occurred in the thymus, where immature thymocytes undergo progressive maturation, before its transferring to spleen and lymph nodes [19]. It has been reported that mice T-cell lymphoma, a model of human T-cell ALL, is induced after radiation exposure during infancy [21, 22]. However, little is known about the B-cell lymphomagenesis by radiation. Therefore, the understanding of radiation-induced ALL provides important insights into the cancer risk assessment by radiation exposure.

In the present study, to investigate the type and differentiation stage of lymphoid tumors induced by ionizing radiation, immunophenotype-based classification was performed on lymphomas developed in gamma-irradiated mice and the risk was estimated for each type of lymphoma (Chapter 1). Then, to elucidate the molecular mechanisms involved in the radiation-induced B-cell lymphoma, genomic profiling of the lymphoma was performed using a next-generation sequencer (Chapter 2).

CHAPTER 1 B-cell lymphomagenesis in mice exposed to ionizing radiation in infancy or young adulthood

1.1 Introduction

Epidemiological studies of atomic bomb survivors in Hiroshima and Nagasaki have revealed a radiation-related increase in the risk of developing solid and hematopoietic tumors [16, 23, 24]. In particular, among atomic bomb survivors, there was a striking effect of radiation exposure on the development of ALL during a short period after exposure [16].

Given the increased use of radiation for medical purposes such as diagnostic imaging and cancer treatment [8], there is great concern about the onset of secondary cancer after radiation exposure. Indeed, the onset of secondary cancers that can be attributed to radiotherapy has been demonstrated in various tissues including skin and breast [25, 26]. In particular, children are thought to be more sensitive than adults to radiation-induced cancers because their organs and tissues are developing [27]. Indeed, it has been reported that a relatively younger age at exposure correlates with increased relative risk for developing leukemias excluding chronic lymphocytic leukemia [28]. In addition, several reports have demonstrated that radiotherapy for primary cancer at young age (i.e., < 21 years of age) has the potential to induce secondary ALL [29, 30].

Lymphoma/leukemia are mainly classified as B-cell and T-cell neoplasms according to immunophenotype, and they are further subclassified as precursor- and mature-cell neoplasms. Previous studies have reported the induction of T-cell lymphomas in mice after radiation exposure in infancy [21, 22]. On the other hand, in a general population, the majority of lymphoid tumors are B-cell lymphoma/leukemia (75%) and

the other tumors are T-cell lymphoma/leukemia, including NK-cell lymphoma/leukemia (5%) and various other known or unknown types (20%) [31]. In addition, it has been reported that the majority of ALLs following radiotherapy at young age are precursor B-cell phenotypes [30]. However, the data concerning the carcinogenic risk associated with each stage of differentiation of B cells after radiation exposure are still insufficient, and the data concerning exposure at young age are particularly scarce.

The aim of the present study was to reveal the effects of age at exposure to radiation on the risk of developing B-cell lymphomas with the precursor- or mature-cell phenotype in mice irradiated with gamma rays in infancy or young adulthood.

1.2 Materials and Methods

1.2.1 Mice and irradiation

F1 hybrid mice were produced by crossing female C57BL/6NCrlCrlj and male C3H/HeNCrlCrlj mice purchased from Charles River Laboratories (Kanagawa, Japan). Certain mice at 3 to 4 days after birth were assigned to three different groups to ensure a similar average body weight among the groups in order to prevent a potential body-weight bias that could possibly influence the carcinogenic effects of radiation exposure [21, 22]. After weaning at 28 days of age, male and female mice were housed separately in aluminum cages (up to five mice per cage), and each cage was changed weekly. Mice were provided with wood-shaving bedding and fed a radiation-sterilized diet (MBR-1: Funabashi Farm Co., Tokyo, Japan) and water ad libitum (water changed twice weekly). The facility was maintained at 23°C ± 3°C with relative humidity 50 ± 10%, a 12-h light-dark cycle and specific-pathogen-free (SPF) condition. Mice at 1 week of age (1W, infancy) or 7 weeks of age (7W, young adulthood) were exposed to a single whole-body dose of 4 Gy gamma rays at 0.5 Gy/min (i.e., at high dose rate) using a ^{137}Cs source (Gammacell-40, Nordion, Ottawa, Canada). Mice were monitored daily, and when they became moribund (abnormal posture, respiratory disorders, anemia, etc.) they were euthanized and autopsied for the analyses below. All experimental procedures were conducted according to the Guidelines for Animal Welfare and Experimentation of the National Institute of Radiological Sciences of Japan (No. 07-1017).

1.2.2 Histopathology

During autopsy, all organs were rapidly fixed with 10% neutral buffered formalin, embedded in paraffin, sectioned transversely at 3- to 4-μm thickness, and stained with

hematoxylin and eosin (HE). Malignant lymphoma including lymphocytic leukemia, were diagnosed by pathologists using J-SHARE (Japan Storehouse of Animal Radiobiology Experiments; NIRS, QST) [32], in which data of autopsy observations and HE specimens prepared by the above methods were registered. A diagnosis of malignant lymphomas (for the determination of the possible cause of death) was assigned to cases that showed disordered proliferation of atypical lymphocytes in bone marrow or lymphoid tissues (thymus, spleen, lymph node, and Peyer's patch), and infiltration of malignant lymphocytes into several lymphoid tissues or organs.

1.2.3 Immunohistochemistry

To classify malignant lymphomas on the basis of immunophenotype, tissue sections were subjected to immunohistochemical staining for lymphoid-cell lineage markers including TdT, PAX5, CD45R, IgM, and CD3 (Table 1) [33]. Sections were subjected to immunostaining for TdT or double immunostaining for CD45R and CD3 using the automated immunostaining apparatus Ventana Benchmark Ultra (Roche Diagnostics, Tokyo, Japan) according to the standard program provided by the manufacturer. Immunostaining for PAX5 and IgM was carried out manually according to standard protocols [34]. All sections were counterstained with hematoxylin.

1.2.4 Classification of malignant lymphomas

Malignant lymphomas were classified into five types on the basis of immunophenotype (Fig. 1) [33]: (i) undifferentiated-cell lymphoma (TdT^+, $Pax5^-$, $CD3^-$, $CD45R^-$), (ii) T-cell lymphoma ($CD3^+$, $Pax5^-$, $CD45R^-$), (iii) pro-B type, poorly differentiated B-cell lymphoma ($Pax5^+$, $CD3^-$, IgM^-), (iv) pre-B type, moderately differentiated B-cell

lymphoma ($CD45R^+$, $CD3^-$, IgM^-), and (v) mature-B type, well-differentiated B-cell lymphoma (IgM^+, $CD3^-$). Malignant lymphomas considered to be mixed (i.e., both $CD45R^+$ cells and $CD3^+$ cells) or double-positive for Pax5 and CD3 could not be definitively classified as B-cell or T-cell lymphoma and thus were classified as unknown type.

1.2.5 Statistical analysis

Differences in the incidence of tumors between sex or groups were analyzed with Fisher's exact test. Mean lifespan differences were analyzed with one-way analysis of variance followed by the post-hoc Tukey test. Mortality attributable to B-cell or T-cell lymphomas was assessed with Kaplan–Meier survival curves, and any statistically significant differences in survival between groups were determined with the log-rank test. Cox proportional hazard analysis of the risk of developing B-cell lymphomas was performed to calculate hazard ratios for radiation exposure in infancy or in young adulthood. Differences in results were considered significant at $P < 0.05$.

Table 1. Summary of immunohistochemical staining methods

Marker	Major positive cells	Antibody	Clone (source)	Epitope retrieval	Dilution	Coloring
TdT[a]	Lymphoblasts of B-cell and T-cell lineage	Rabbit-anti human polyclonal	- (Spartech's)	HIER[b] with Tris-EDTA (pH 8.5)	1:50	DAB[c]
Pax5	Pro-B cell, pre-B cell, and B-cell	Rabbit-anti mouse monoclonal	3852-1 EPR3730(2) (Abcam)	HIER with Citrate buffer (pH 7.0)	1:500	DAB
CD45R[a,d] (B220)	Pre-B cell and B-cell	Rat-anti mouse monoclonal	RA3-6B2 (BD Biosciences)	HIER with Tris-EDTA (pH 8.5)	1:50	DAB
IgM	B-cell	Rat-anti mouse monoclonal	II/41 (Novus Biologicals)	EIER[e] with Proteinase-K	1:200	DAB
CD3[a,d]	T-cell lineage	Rabbit-anti mouse monoclonal	SP7 (Abcam)	HIER with Tris-EDTA (pH 8.5)	1:150	Fast red

[a] Semi-automatic staining with the Ventana benchmark ultra.

[b] HIER, heat-induced epitope retrieval method.

[c] DAB, 3',3'-diaminobenzidine.

[d] Double staining.

[e] EIER, enzyme-induced epitope retrieval method.

1.3 Results

1.3.1 Effects of radiation exposure on the incidence of malignant lymphoma in mice

Fig. 1 presents representative images of HE and immunohistochemical staining of malignant lymphomas. Malignant lymphomas were diagnosed by HE-stained specimens of mouse tissues including spleen and thymus, followed by confirmation of positive staining for lymphoid markers (i.e., TdT, Pax5, IgM, CD3 and CD45). As shown in Fig. 2, the incidence of malignant lymphomas was 61% (34 of 56) and 36% (18 of 50) for non-irradiated female and male mice (control), respectively, implying significantly higher incidence of lymphomas in female than male mice. The incidence of lymphomas was 38% (19 of 50) for both female mice irradiated in infancy (1W) or young adulthood (7W), and they were significantly lower than that of the non-irradiated female mice (Fig. 2A). On the other hand, the incidence of lymphomas was 42% (20 of 48) and 34% (17 of 50) in male mice in the 1W and 7W groups, respectively, and no significant difference in the incidence of lymphomas was observed between the irradiated and non-irradiated groups (Fig. 2B). These results suggest that malignant lymphomas spontaneously occur with high frequency in B6C3F1 mice, especially in female mice, and that exposure to radiation does not increase the overall incidence.

1.3.2 Effects of radiation exposure and age at exposure on the incidence of each type of malignant lymphoma in mice

Based on the immunophenotype, malignant lymphomas were classified into five types: undifferentiated-cell lymphoma (TdT^+, $Pax5^-$, $CD3^-$, $CD45R^-$), T-cell lymphoma ($CD3^+$, $Pax5^-$, $CD45R^-$), pro-B type-B-cell lymphoma ($Pax5^+$, $CD3^-$, IgM^-), pre-B type-B-cell

lymphoma ($CD45R^+$, $CD3^-$, IgM^-), and mature-B type-B-cell lymphoma (IgM^+, $CD3^-$) (Fig. 1). The incidence of each lymphoma is also shown in Fig. 2. The female mice in the control group had 2%, 39%, and 16% (1, 22 and 9 of 56) incidence of the pro-B, pre-B, and mature-B type lymphomas, respectively, as well as no incidence of undifferentiated-cell or T-cell lymphomas (Fig. 2A). Among female mice in the 1W group, the incidence of T-cell lymphoma (20%, 10 of 50) was significantly higher than in the control group (0%, 0 of 56). On the other hand, the incidence of pre-B (14%, 7 of 50) and mature-B type (0%, 0 of 50) lymphomas was significantly lower than that in the control group. Likewise, the incidence of pre-B type lymphoma (20%, 10 of 50) among female mice in the 7W group was significantly lower than that in the control group.

Male mice in the control group had 2%, 30%, and 2% (1, 15 and 1 of 50) incidence of the pro-B, pre-B, and mature-B type lymphomas, respectively, as well as no incidence of undifferentiated-cell or T-cell lymphomas (Fig. 2B). Among male mice in the 1W group, the incidence of T-cell lymphoma (29%, 14 of 48) was significantly higher than in the control group. On the other hand, the incidence of pre-B lymphomas in the 1W group (8%, 4 of 48) was significantly lower than that in the control group. There were no significant differences in the incidence of each lymphoma in male mice between the 7W and control groups. These results suggest that radiation exposure in infancy induces T-cell lymphoma in both female and male mice, resulting in decreased incidence of pre-B and mature-B type lymphomas.

1.3.3 Effects of radiation exposure on the age at death owing to B-cell and T-cell lymphomas in mice

Table 2 presents data for the overall lifespan of the mice used in the present study. Radiation exposure significantly reduced lifespan, regardless of age at exposure. This observation suggested that malignant lymphomas, which was the major cause of death in these mice (Fig. 2), developed immediately after irradiation. Therefore, the lifespan of the mice with malignant lymphomas was analyzed. In female mice, the B-cell lymphomas–free survival rate of the control group began to decrease at 616 days after birth (Fig. 3A). For the 1W and 7W groups, B-cell lymphomas–free survival rate decreased between 200 to 287 days and 282 to 412 days, respectively, after birth (early onset of B-cell lymphoma) and, after a plateau period, it began to decrease again after 535 days and 674 days (late onset of B-cell lymphoma), respectively. The B-cell lymphomas–free survival curves revealed significant differences between the 1W or 7W group and the control group. In addition, the death rate due to late-onset B-cell lymphomas significantly increased in the 1W and 7W groups, compared with that due to spontaneous B-cell lymphomas in the control group.

Likewise, in male mice, the B-cell lymphomas–free survival rate of the control group began to decrease at 510 days after birth (Fig. 3B). For the 1W group, B-cell lymphomas–free survival rate decreased between 170 and 346 days after birth (early onset of B-cell lymphoma) and, after a plateau period, it began to decrease again after 578 days (late onset of B-cell lymphoma). In contrast, for the 7W group, early onset of B-cell lymphoma was not observed, and the B-cell lymphomas–free survival rate decreased after 510 days (late onset of B-cell lymphoma). The B-cell lymphomas–free survival curves revealed a significant difference between the 7W group and the control group. The increase in the death rate due to late-onset B-cell lymphomas in the 7W group, compared with that due to spontaneous B-cell lymphomas in the control group, was also observed

in male mice. Although the mean lifespan of irradiated mice that died from late-onset B-cell lymphoma was not significantly different from control mice that died from spontaneous B-cell lymphoma, the mean lifespan of irradiated mice that died from early-onset B-cell lymphoma was significantly shortened compared with control mice that died from spontaneous B-cell lymphoma (Table 3).

Furthermore, the survival curves stratified by the type of B-cell lymphoma were analyzed. Early-onset pro-B type lymphoma was observed in both the 1W and 7W groups (except for the male mice in the 7W group), and survival curves revealed a significant difference between the 7W group and the control group (Fig. 4A and D). Early-onset pre-B type lymphoma was also observed in both the 1W and 7W groups (except for the male mice in the 7W group), and survival curves revealed a significant difference in female mice between the 1W or 7W and control groups and in male mice between the 7W and control groups (Fig. 4B and E). In contrast, early-onset mature-B type lymphoma was not observed, and no significant differences in survival curves were observed in both female and male mice among the three groups (Fig. 4C and F). Collectively, these results suggested that radiation exposure accelerates the onset of the pro-B and pre-B type lymphomas. In addition, data for age at death due to pro-B or pre-B-type lymphomas after radiation exposure revealed a bimodal distribution, i.e., mice could be classified as short- or long-lived.

On the other hand, as shown in Fig. 5, T-cell lymphoma–free survival rate decreased between 106 to 348 days and 198 to 226 days in female mice in the 1W and 7W groups, respectively, and the survival curves revealed significant differences between the 1W and control or 7W group. Likewise, in male mice, T-cell lymphoma–free survival rate decreased between 86 to 682 days and 215 to 387 days in the 1W and 7W groups,

respectively, and the survival curves revealed significant differences between the 1W and control or 7W groups. In addition, T-cell lymphoma was induced significantly earlier than late-onset B-cell lymphoma in the 1W and 7W groups, except for the male mice in the 1W group (Table 3). The induction of T-cell lymphomas in male mice in the 1W group also showed a trend toward earlier than late-onset B-cell lymphoma (P=0.08) (Table 3), due to the fact that several T-cell lymphoma–bearing mice died relatively late (Fig. 5). Consistent with previous reports using infant mice [21, 22], these data suggest that radiation exposure in infancy rapidly and predominantly induces T-cell lymphomas.

1.3.4 Difference in risk of each type of B-cell lymphoma by age at exposure

Next, the hazard ratios were calculated for malignant lymphomas by radiation exposure. Notably, however, no T-cell lymphoma occurred in the control group (Fig. 2), thus preventing the calculation of hazard ratios for T-cell lymphomas. Fig. 6 presents hazard ratios for each type of B-cell lymphoma in the 1W and 7W groups versus the control group. In female mice in the 1W group, the overall hazard ratio for B-cell lymphomas was 4.0 (1.6–9.8) (Fig. 6A). In particular, hazard ratio for pre-B type lymphoma was 4.4 (1.6–12), implying a significant carcinogenic risk associated with radiation exposure. In addition, although the early-onset pro-B type lymphoma was observed in the 1W group, no significant carcinogenic risk was observed for pro-B type lymphoma, perhaps due to the low incidence of the lymphoma. Furthermore, in the 7W group, the overall hazard ratio of B-cell lymphoma was 2.9 (1.5–5.7). In particular, the hazard ratios for the pro-B and pre-B types were 17.5 (1.9–158.9) and 2.4 (1.1–5.4), respectively, implying a significant carcinogenic risk associated with radiation exposure. No significant carcinogenic risk was observed for mature-B type lymphoma.

In contrast, in male mice in the 1W group, no significant carcinogenic risk was observed for B-cell lymphomas (Fig. 6B). In the 7W group, the overall hazard ratio for B-cell lymphomas was 3.7 (1.6–8.5). In particular, the hazard ratio for pre-B type lymphoma was 2.6 (1.0–6.4), implying a significant carcinogenic risk associated with radiation exposure. Notably, all male mice in the 7W group died before the pro-B or mature-B type lymphoma–bearing mice in the control group died (Fig. 4D and F), thus preventing the calculation of hazard ratios for pro-B or B-cell lymphoma. Collectively, these results suggested that radiation exposure in infancy increases the risk of developing pre-B type lymphoma only in female mice. On the other hand, the present data suggest that young adulthood exposure increases the risk of developing B-cell lymphomas (particularly pro-B or pre-B type lymphomas), and this risk is greater in male mice than female mice.

Table 2. Experimental design and overall lifespan of mice

Group	Age at irradiation	Dose (Gy)	Sex	Number of mice	Overall lifespan [a]
Control	Non-irradiated	0	Female	56	846 ± 139 (345–1210)
			Male	50	829 ± 202 (149–1179)
1W	1 week	4	Female	50	475 ± 246 (78–864) *
			Male	48	505 ± 279 (86–1208) *
7W	7 weeks	4	Female	50	620 ± 206 (198–955) *
			Male	50	635 ± 177 (215–941) *

[a] Mean lifespan in days ± SD. Values in parentheses are the minimum and maximum.

*Indicates a significant difference versus the control group ($P < 0.05$, one-way analysis of variance followed by post-hoc pairwise Tukey's test).

Table 3. Mean lifespan (days ± SD) of B-cell or T-cell lymphomas-bearing mice

	Female			Male		
	Control	1W	7W	Control	1W	7W
B-cell lymphomas						
Spontaneous	862 ± 108 (32[a]) (616–1117[b])	ND	ND	894 ± 140 (17) (688–1163)	ND	ND
Early-onset	ND	244 ± 62 (2)[*] (200–287)	337 ± 67 (3)[*] (282–412)	ND	260 ± 88 (3)[*] (170–346)	ND
Late-onset	ND	724 ± 117 (7)[†] (535–864)	772 ± 86 (14)[†] (674–955)	ND	672 ± 133 (2) (578–766)	733 ± 136 (13)[†] (510–941)
T-cell lymphomas	ND	216 ± 82 (10) (106–348)	212 ± 20 (2) (198–226)	ND	249 ± 165 (14) (86–682)	298 ± 86 (3) (215–387)

[a]The numbers of tumor-bearing mice are shown in parentheses on the upper rows.

[b]The minimum and maximum lifespans of B-cell or T-cell lymphoma-bearing mice are shown in parentheses on lower rows.

[*]Indicates a significant difference versus B-cell lymphomas in the control group.

[†]Indicates a significant difference versus T-cell lymphoma.

ND, not diagnosed.

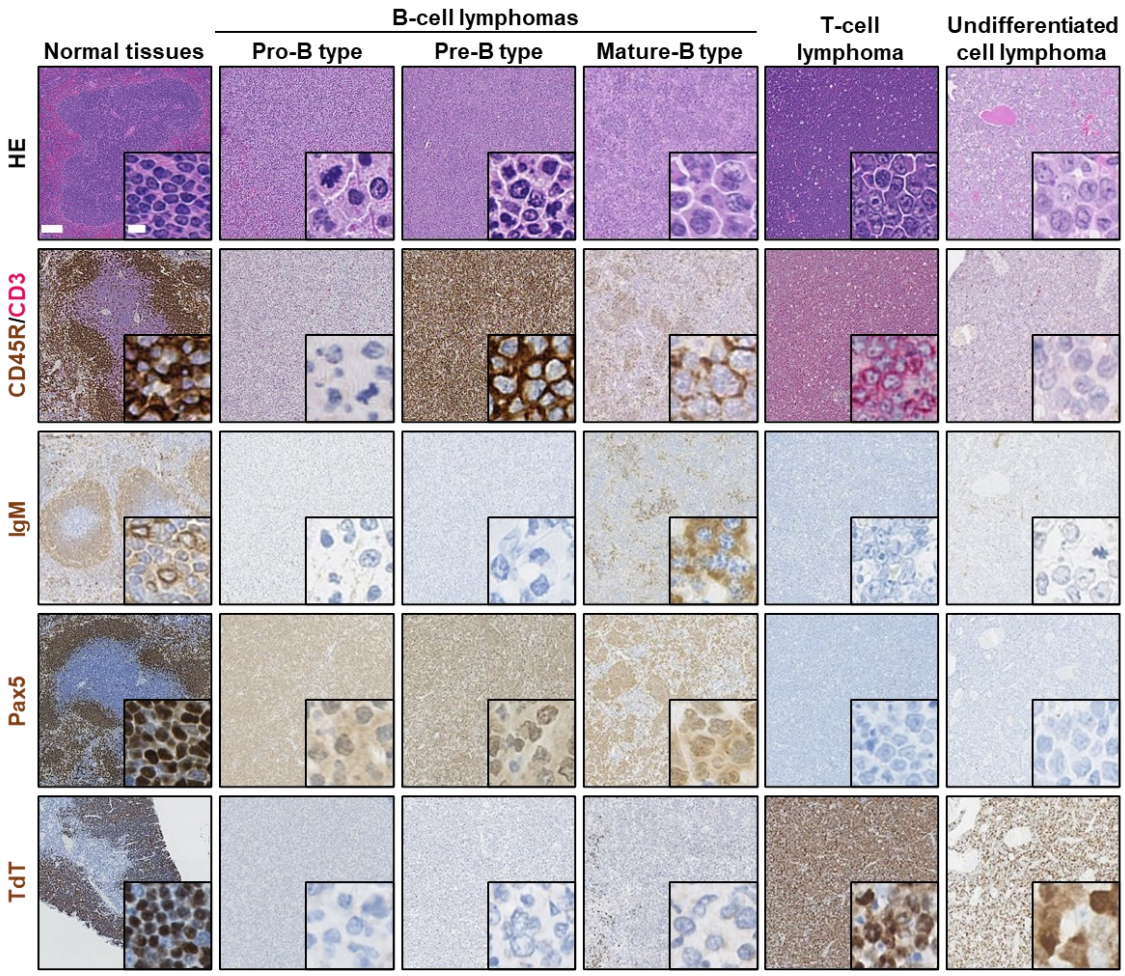

Figure 1. Histopathology and immunohistochemistry of lymphomas resected from mice. Each tumor was diagnosed by conventional HE staining. Malignant lymphomas were classified as either undifferentiated-cell or being of B-cell or T-cell origin based on immunohistochemistry. Each B-cell lymphomas were further classified as the pro-B, pre-B, or mature-B type. As a positive control, normal spleen was stained for CD45R/CD3, IgM and PAX5, and normal thymus was stained for TdT. Shown are representative images of normal lymphoid tissues (spleen or thymus) and malignant lymhpmas that had been subjected to HE staining and immunohistochemical staining for CD45R/CD3, IgM, PAX5 and TdT. All images were acquired at the same magnification. Scale bar, 100 μm (5 μm in the inset).

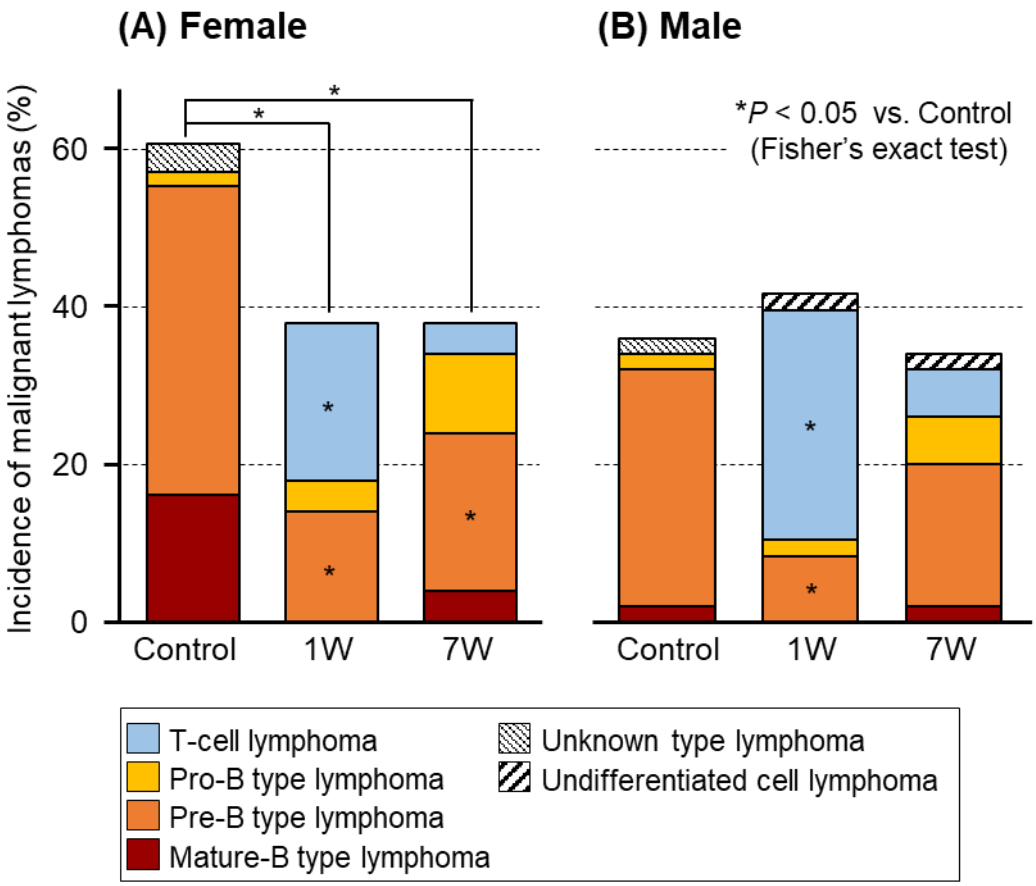

Figure 2. Incidence of each type of malignant lymphomas in (A) female and (B) male mice in the control, 1W and 7W groups. Each asterisk denotes a significant difference from the control ($P < 0.05$, pairwise Fisher's exact test followed by the m×n x^2-square test).

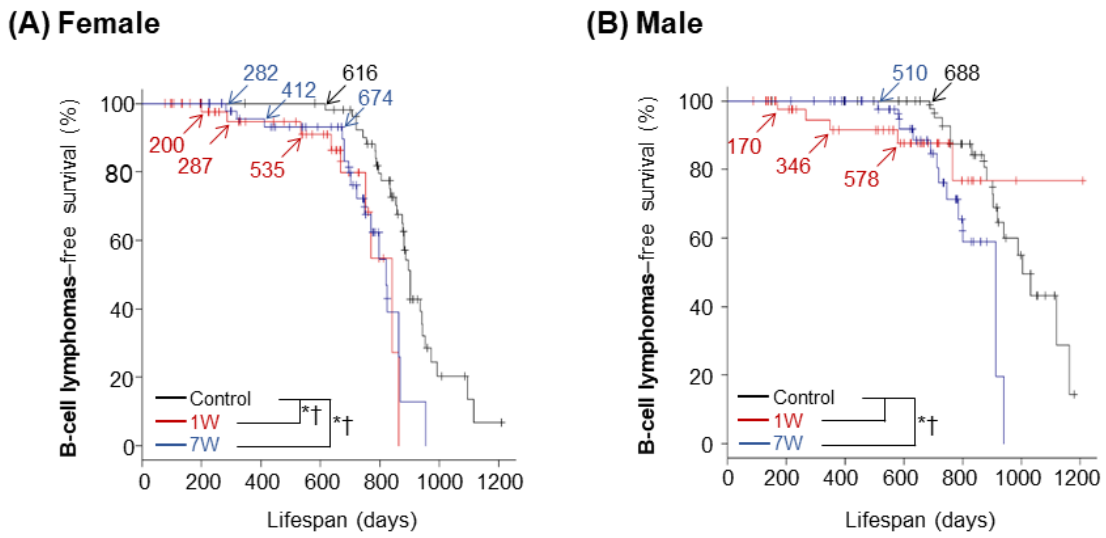

Figure 3. Overall B-cell lymphomas–free survival of (A) female and (B) male mice in the three groups. Kaplan–Meier curves are shown. Asterisks or daggers denote significant differences between curves during the overall period or late-onset B-cell lymphomas- occurring period.

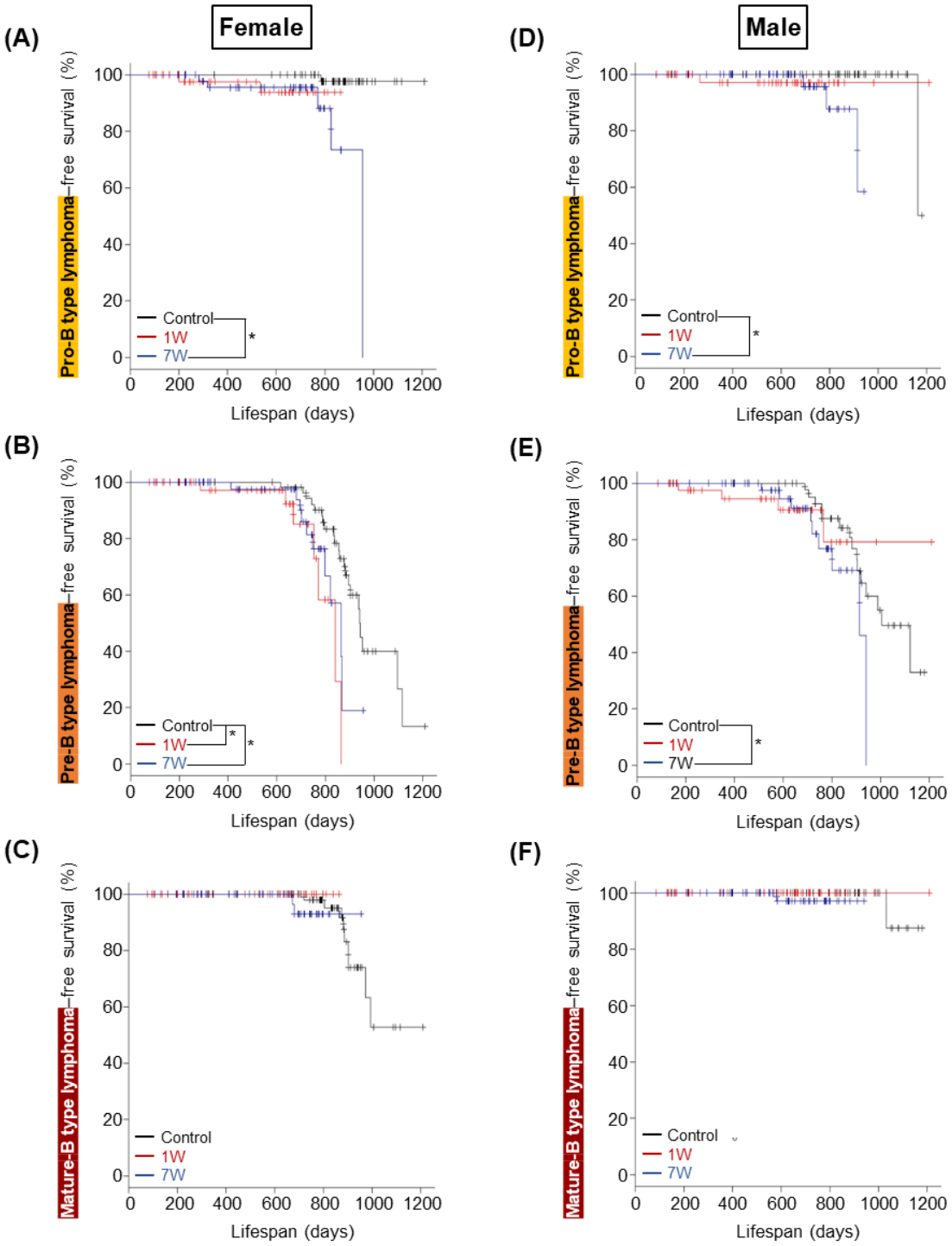

Figure 4. Each B-cell lymphoma–free survival of (A–C) female and (D–F) male mice in the three groups. Kaplan–Meier curves are shown. (**A** and **D**) Pro-B type. (**B** and **E**) Pre-B type. (**C** and **F**) Mature-B type. Asterisks denote significant differences between curves.

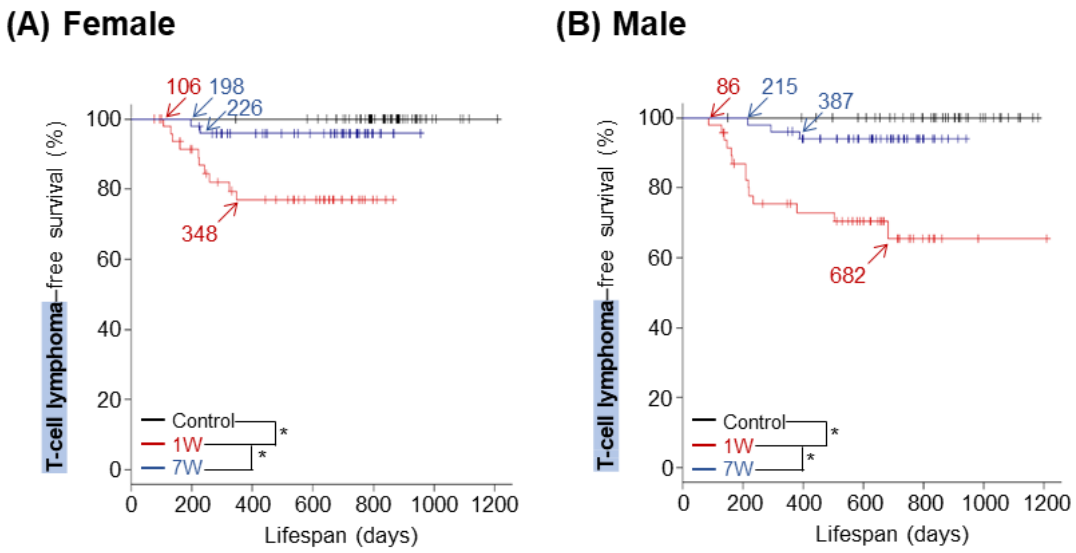

Figure 5. T-cell lymphoma–free survival of (A) female and (B) male mice in the three groups. Kaplan–Meier curves are shown. Asterisks denote significant differences between curves.

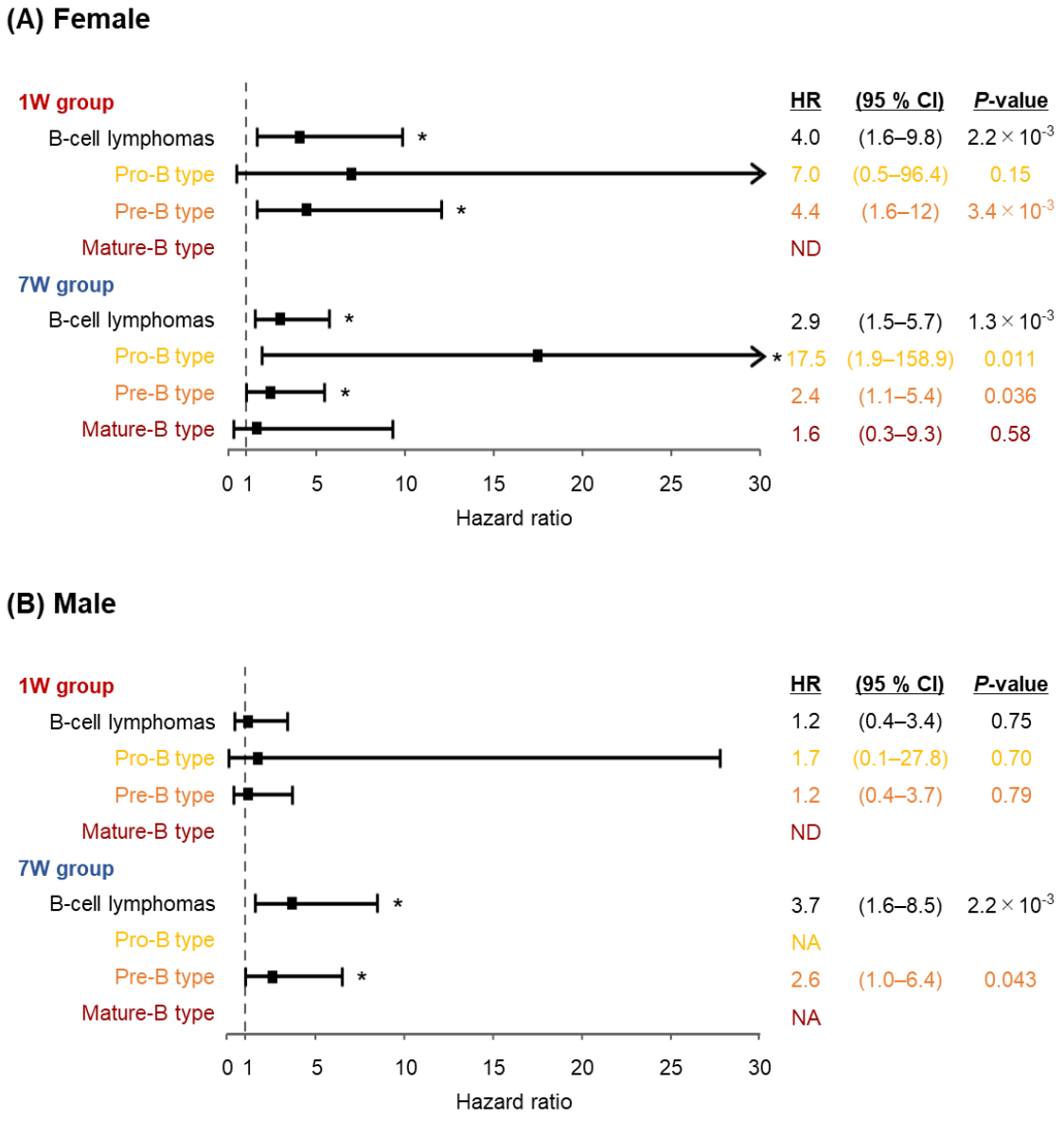

Figure 6. Cox proportional hazard analysis of B-cell lymphomas in (A) female and (B) male mice. Each asterisk denotes a significant difference from the control ($P < 0.05$). HR, hazard ratio; 95 % CI, 95 % confidence interval; ND, not diagnosed; NA, not applicable.

1.4 Discussion

To reveal the effects of radiation exposure at young age on the development of B-cell neoplasms, the carcinogenic risk on B-cell lymphomas was investigated using B6C3F1 mice irradiated with gamma rays at 1 or 7 weeks of age. In mice, the major site of hematopoiesis has already shifted from fetal liver to bone marrow by 1 week of age [35], and this period is analogous to infancy in humans, i.e., ≤1 year of age [36]. On the other hand, in 7-week-old mice, hematopoiesis is carried out in the bone marrow at the same time as sexual maturation and a rapid increase in body weight [22], and this period is analogous to young adulthood in humans, i.e., age range of approximately 12–21 years [36].

In the present study, a high incidence of B-cell lymphomas was observed in the control group, especially in female mice (Fig. 2). Consistent with the previous lifespan study, it has been reported that aged B6C3F1 and C57BL/6 (parent of B6C3F1) mice spontaneously develop lymphomas—most of which are B-cell lymphomas—with high frequency, and the incidence of the lymphomas is higher in female mice than male mice [37]. Although the genetic backgrounds that lead to the high incidence of spontaneous lymphomas in these mice strains are still unknown, the high proportion of B-cell lymphomas seen in these mice is similar to that seen in humans. These mice strains are widely used as a model of human lymphoma and leukemia due to their histopathological and genetic similarities [21, 22, 37-40]. Therefore, the B6C3F1 mice used in the present study are a suitable model to investigate differences in the age of onset and the frequency of each immunophenotype (i.e., pro-B, pre-B and mature-B type) of B-cell lymphomas developed spontaneously or after irradiation.

In the present study, death attributable to precursor B-cell (pro-B and pre-B type) lymphomas after radiation exposure during young adulthood (7W) occurred in mice at a younger age compared with the control group (Figs. 4 and 6). In addition, the risk of developing precursor B-cell lymphomas was increased by radiation exposure during young adulthood, and this was particularly the case for the pro-B type lymphoma. Furthermore, the hazard ratio of developing B-cell lymphomas was relatively higher in male mice than female mice in the 7W group (Fig. 6). Consistent with present results, an epidemiological study of atomic bomb survivors revealed that the risk of developing ALL was high at younger-attained age [16], although the study does not investigate the immunophenotype (i.e., precursor B or T) of the tumors. In addition, in the same study, the risk of developing ALL was higher in male survivors compared with female survivors [16]. It has also been reported that the onset of pro-B ALL is frequently observed in patients following radiotherapy for primary cancers [41]. Thus, these results suggest that radiation exposure during young adulthood accelerates the development of precursor B-cell lymphomas, resulting in an increased risk, despite the decreased incidence of the lymphoma.

Although early-onset precursor B-cell lymphomas were observed in both female and male mice after radiation exposure in infancy (1W) (Fig. 4), the significant carcinogenic risk was observed only in the pre-B type lymphoma in female mice (Figs. 4 and 6). Interestingly, consistent with this result, the risk of developing pre-B ALL is slightly increased in patients who have exposed to diagnostic X-rays at less than 15 years old [42]. In accord with previous reports [21, 22], mouse T-cell lymphoma was also induced immediately after radiation exposure in infancy with high frequency, and the incidence was higher in male than female. Consistent with this, a potential increase in the

incidence of T-cell ALL has also been reported for patients who have undergone radiation therapy for cancer at less than 18 years old [30]. However, the majority of ALL developed in the patients were precursor B-cell leukemia [30]. Therefore, present results suggest that T-cell lymphoma is preferentially induced by radiation if a high-dose exposure occurs in infancy (such as cases of accidental radiation exposure). On the other hand, in mice it has been reported that regeneration of the thymus after high-dose irradiation precedes that of bone marrow and spleen, and subsequently, T-cell lymphoma (i.e., thymic lymphoma) develops from the irradiated thymocytes [43, 44]. Moreover, it has been reported that radiation-induced T-cell lymphoma occurs primarily in young mice rather than old mice, possibly reflecting a difference in the thymic microenvironment of age at exposure [45]. In the present study, a large number of mice in the 1W group, particularly male mice, also died due to the rapid induction of T-cell lymphoma and therefore the proportion of mice survived until the late period (after 510 days of age) was smaller than in the control group with no induction of T-cell lymphoma (Fig. 5). This leads to a lower incidence of late-onset pre-B type lymphoma in the 1W group compared to the control group (Fig. 4). This scenario suggests no statistically significant risk for developing pre-B type lymphoma in male mice after radiation exposure in infancy (Fig. 6). Thus, the results suggest that radiation exposure in infancy potentially increases the carcinogenic risk of precursor B-cell lymphomas, not just for the pre-B type lymphomas in females. On the other hand, it is suggested that a significantly shortened average lifespan of mice in the 1W group compared to the control group (Table 2) is due to the death of the large proportion of mice from B-cell or T-cell lymphoma in the 1W group before the death of the majority of mice in the control group (after 600 days of age) (Figs. 3 and 5).

In contrast to the observed risk of precursor B-cell lymphomas, no increase in the risk of mature B-cell lymphoma was observed in mice after radiation exposure (Fig. 6). Indeed, it has been reported that mature B-cell lymphomas, which constitute the majority of non-Hodgkin lymphomas in humans [31], rarely occur in patients after radiotherapy [46]. On the other hand, in the study of atomic bomb survivors, the excess relative risk of non-Hodgkin lymphoma is reported among young male survivors, although the evidence of a radiation dose response is weak [16]. In the study, however, the types of lymphoma (i.e., precursor B-cell, mature B-cell, T-cell or others) were not investigated. Present results suggest that the observed increased risk of developing non-Hodgkin lymphomas after radiation exposure is due to the early induction of precursor B-cell and T-cell lymphoma and leukemia in humans. The data hypothesize that radiation-induced precursor B-cell lymphomas are the result of malignant transformation of precursor B cells or undifferentiated hematopoietic cells (i.e., stem cells) by radiation. Indeed, it has been reported that chromosomal deletion including a tumor-suppressor gene was observed in the multipotent progenitor cells in a radiation-induced acute myeloid leukemia mouse model [47].

The present study found that the age at death due to precursor-B cell lymphomas in irradiated mice showed bimodality at both the early (before 412 days of age) and late (after 510 days of age) periods (Table 3 and Figs. 3 and 4). In addition, spontaneous B-cell lymphomas were not observed during the early period, and development of B-cell lymphomas in irradiated mice (i.e., late-onset B-cell lymphomas) was significantly accelerated during the late period compared to development of spontaneous B-cell lymphomas. According to the findings from epidemiological studies, the mechanisms involved in the onset of radiation-induced leukemia are hypothesized to differ with

respect to whether the disease is early- or late-onset [24, 48]. That is, early-onset leukemia may be a consequence of transformation of pre-leukemic cells induced by sporadic genomic aberrations that, upon acquisition of additional radiation-induced gene mutations, result in malignant cells [48]. In contrast, late-onset leukemia may develop as a consequence of the acquisition of genomic abnormalities, including gene mutations caused by radiation exposure in normal hematopoietic cells [24]. Therefore, while both early- and late-onset precursor B-cell lymphomas in mice are possibly induced by radiation exposure, their underlying carcinogenic mechanisms may be different.

The present study indicates that radiation exposure induces precursor B-cell lymphoma and leukemia immediately after exposure if it occurs at young age, especially in young adulthood, resulting in an increased risk. These results provide valuable information regarding the risk assessment of lymphoma and leukemia following exposure to ionizing radiation.

CHAPTER 2 Molecular mechanisms of radiation-induced mouse precursor B-cell lymphomas

2.1 Introduction

Precursor B-cell acute lymphoblastic leukemia (B-ALL) is the most common childhood cancer accounting for about 80% of all ALL cases and it comprises multiple subtypes with different genetic alterations that are important for risk stratification [18, 49]. The B-ALL subtypes are characterized by aneuploidy, chromosomal rearrangements leading to the expression of fusion oncogenes (e.g., *ETV6-RUNX1*, *BCR-ABL1*, *TCF3-PBX1*), and certain ALL-specific genomic profiles such as *BCR-ABL1*-like (known as Philadelphia chromosome [Ph]-like) and *ETV6-RUNX1*-like [50]. In addition, B-ALL cases are categorized by genetic alterations in lymphoid transcription factors (*IKZF1, PAX5, EBF1,* and *ETV6*), cell cycle regulators and tumor suppressors (*CDKN2A/B, TP53,* and *RB1*), regulators of lymphoid signaling (*BTLA* and *CD200*), Ras pathway signaling (*NRAS, KRAS,* and *PTPN11*), and chromatin modifiers (*CREBBP, SETD2,* and *WHSC1*) [50].

Ionizing radiation is an established risk factor of ALL, as evidenced by numerous epidemiological studies. Particularly, leukemia, including ALL, was the earliest cancer observed among the atomic-bomb survivors [4]. In addition, several studies have reported the development of B-ALL following exposure to radiation used in medical applications such as diagnostic imaging and cancer treatment [30, 42]. However, the genetic alterations of radiation-induced B-ALL have not been elucidated. It is also important to clarify the genomic abnormalities characteristic of radiation-induced B-ALL, which enables to distinguish between radiation-induced and spontaneous B-ALLs and are useful for prevention/treatment of radiation-induced B-ALL.

As described in the Chapter 1, the present study revealed the early induction of precursor B-cell lymphoma in mice irradiated with gamma-rays during infancy or young adulthood compared with non-irradiated mice. Thus, the aim of the present study was to identify the genetic basis involved in the early-onset mouse B-cell lymphomas developed after radiation exposure.

2.2 Materials and Methods

2.2.1 Tumor samples

B-cell lymphomas were excised from irradiated (n = 21) and non-irradiated (n = 11) mice as described in the Chapter 1, and samples were stored at –80°C.

2.2.2 Whole-exome sequencing

Genomic DNA and total RNA were co-isolated from lymphomas and ears of mice using the AllPrep DNA/RNA/Protein Mini kit (Qiagen, Hilden, Germany). Extracted DNA was then treated with RNase and purified using the QIAmp DNA Micro kit (Qiagen). DNA was quantified using a Qubit fluorometer (Life Technologies, Tokyo, Japan), and 3 μg DNA was sheared into fragments (~150–200 bp) using the Covaris S220 system. Exon capture was performed with the SureSelect Mouse All Exon V2 kit (Agilent Technologies, Santa Clara, CA, USA). Exon capture libraries were sequenced using the 75-bp paired-end protocol of a NextSeq sequencer (Illumina, Tokyo, Japan), generating an average of 72 million quality-filtered reads per sample.

2.2.3 Exome data analysis

Somatic mutations were detected using a pipeline developed by Amelieff (Tokyo, Japan) as previously described [39]. Briefly, the reads were trimmed by removing low-quality bases and discarded if they were shorter than 32 bases or if >80% of any individual read had a quality rating of <20 using the QCleaner tool. Reads were aligned to the mouse reference genome (mm10) using the Burrows-Wheeler Alignment tool. Duplicate reads were removed with SAMtools (version 1.2), and base quality recalibration and realignment around insertions/deletions were performed using the Genome Analysis Tool

kit. Somatic single-nucleotide variants and insertions/deletions in tumors were called with VarScan 2 software (version 2.4.3) [51]. A false-positive filter was then applied to remove sequencing- or alignment-related artifacts. Variants were annotated and the effect on coding sequences predicted using SnpEff software (version 4.3) [52]. Variant alleles were excluded from the dataset if they were present in fewer than 10% of tumor reads or had no normal reads. Control-FREEC software (version 10.8) [53] was used to identify copy-number changes in tumors compared with normal tissue.

2.2.4 Array comparative genomic hybridization (array-CGH)

DNA copy-number aberrations across the lymphoma genome were assessed using array comparative genomic hybridization, which was performed using the Mouse Genome CGH Microarray kit (Agilent Technologies). Fluorescent labeling of DNA, microarray hybridization, and post-hybridization washing were conducted per the Agilent protocol. The array images were scanned using an Agilent Microarray Scanner (G2565CA), and signal intensities were measured with Feature Extraction software ver. 10.5.1. Copy-number variations were identified using the Genomic Workbench Lite Edition 7.0 (Agilent Technologies) with probe-quality weighted interval scores (ADM-2, Threshold = 7.5) after excluding probes with saturated signals and default normalization and centralization of the data. The microarray data were deposited in the Gene Expression Omnibus database (www.ncbi.nlm.nih.gov/geo) under accession number GSE192455.

2.2.5 Target sequencing

First-strand complementary DNA was synthesized from 1 μg total RNA using SuperScript III reverse transcriptase (Thermo Fisher Scientific, Waltham, MA, USA), except for two

samples (cases 9 and 25) for which the RNA had degraded. The exon regions of *Jak3* were amplified from cDNA by PCR using primer sequences listed in Table 4. After agarose gel electrophoresis, amplified fragments were excised, eluted from gel pieces using the Freeze-N-Squeeze Spin Column (Bio-Rad Laboratories, Hercules, CA), and purified by ethanol precipitation. Subsequently, sequencing was performed using the primers and Big Dye Terminator v3.1 kit (Thermo Fisher Scientific) and then analyzed on a 3500xL Dx Genetic Analyzer (Thermo Fisher Scientific).

2.2.6 Quantitative PCR analysis

The synthesis of cDNA was carried out as described above. To examine the expression of *Pax5*, *Cd19* and *Blnk*, quantitative reverse transcription-PCR was performed using the LightCycler system (Roche, Basel, Switzerland) with SYBR Premix Ex Taq (Takara Bio, Shiga, Japan) and the primers listed in Table 4. Expression data were normalized to values obtained for the housekeeping gene *Gapdh*.

2.2.7 RNA sequencing (RNA-seq)

Total RNA was isolated as described above. RNA-seq was performed by GENEWIZ (Tokyo, Japan) on the DNBSEQ-G400 platform. Gene expression values (raw read counts) from BAM files were calculated using StrandNGS (version 4.0). The RPKM algorithm using default values was selected. The expression data of transcripts were filtered based on their normalized RPKM values (within the 20^{th} to 100^{th} percentile). Differentially expressed genes (≥2-fold, $P < 0.05$) between lymphoma groups were then identified by a moderate *t*-test followed by Benjamini and Hochberg multiple test correction for each gene. Hierarchical clustering and Gene Ontology analyses were

performed for the differentially expressed genes. Normalized data were subjected to gene-set enrichment analysis using the program GSEA (version 4.1.0) [54]. For detection of fusion transcripts, RNA-seq data were analyzed with STAR-Fusion software (version 1.4.0) [55]. The data were deposited in the Gene Expression Omnibus database under accession number GSE191221.

2.2.8 Western capillary electrophoresis

Total protein was extracted from lymphomas using cell lysis buffer (Cell Signaling, Danvers, MA, USA; #9803) followed by boiling in SDS-PAGE sample buffer. The concentration of the total protein was determined using the BCA (bicinchoninic acid) Protein Assay kit (Thermo Fisher Scientific). Simple western analysis (capillary electrophoresis-based immunodetection) was performed on a Wes system (ProteinSimple, Tokyo, Japan) [56] using the 12–230kDa Jess/Wes Separation Module (ProteinSimple). Total protein, loaded at a concentration of 1.0 mg/ml or 0.25 mg/ml (prepared by diluting 1.0 mg/ml samples), was separated through a size-resolving matrix in the capillaries, immobilized to the inner capillary wall, and then incubated with the first antibody against Stat5 (Cell Signaling; #9359), phospho-STAT5 (pStat5; Cell Signaling; #84205), or β-actin (Cell Signaling; #4967). Following these steps, samples were incubated with anti-rabbit secondary antibody (ProteinSimple) followed by detection of each target protein using chemiluminescence. Band intensities were quantified by determining the area under curve for Stat5 or pStat5 in each sample using Simple Western Compass Software (ProteinSimple), and the values were normalized to that for β-actin.

2.2.9 Immunohistochemistry

Formalin fixed paraffin embedded tissues from mice were sectioned transversely at 3- to 4-μm thickness and subjected to immunostaining for Pax5 as described in the Chapter 1.

Table 4. Primer sets for quantitative PCR and target sequencing

Target	Direction	Sequence (5'→3')
Gapdh	Forward	GCGAGACCCCACTAACATCAA
	Reverse	TGGTTCACACCCATCACAAAC
Pax5 (exon2-3 region)	Forward	CCAGATGTAGTCCGCCAAAGG
	Reverse	ATGCTTCCTGTCTCATAATACCTGC
Cd19	Forward	AGGCACCTATTATTGTCTCCGAGG
	Reverse	ATCCACCAGTTCTCAACAGCCA
Blnk	Forward	AGCCGTACACCCTAGTTGCG
	Reverse	TTGACGATTTCCACAACACTTCCG
Jak3 (c.1958 and 2009)	Forward	GATGGTGGACACATGACTCGGA
	Reverse	CCCCACTTGTCAGCCTCCAA
Jak3 (c.2507 and 2531)	Forward	AGCTCCTCTCAGACCCCACA
	Reverse	TAGCTGACTCCCCGGTACTTGA

2.3 Results

2.3.1 Characterizing the genetic alterations of B-cell lymphoma that develop in irradiated mice

The study, described in the Chapter 1, revealed that B6C3F1 mice irradiated with 4 Gy of gamma-rays develop B-cell lymphoma with bimodal incidence, peaking in the early and late periods (before 60 and after 70 weeks of age, respectively), whereas non-irradiated mice spontaneously develop B-cell lymphoma after 90 weeks of age [57]. To profile the somatic mutation spectrum of radiation-induced B-cell lymphomas, whole-exome sequencing was conducted on three types of mouse B-cell lymphomas (obtained in the study described in the Chapter 1): i) early-onset B-cell lymphomas (n = 6) and ii) late-onset B-cell lymphomas (n = 15), which developed in the irradiated mice, and iii) spontaneous B-cell lymphomas (n = 11), which developed in non-irradiated control mice. The number of mutations did not differ significantly between the three types of B-cell lymphomas (Fig. 7). Among the genes that were identified as having non-synonymous mutations and/or copy-number aberrations, further analysis identified the genes which were annotated as drivers of human hematopoietic tumors in the human cancer database [58] (Fig. 8). Copy-number gain of *Myc* was the most frequent genomic alteration (34% of cases) among all B-cell lymphomas (Fig. 8). Notably, six genes (*Jak3*, *Pax5*, *Jak1*, *Sh2b3*, *Ccnc*, *Ptpn11*) had a high frequency (i.e., ≥20% of cases) of abnormalities in the early-onset precursor B-cell lymphomas. Among them, mutations in *Jak3* within its pseudokinase domain (R653H and V670A) or kinase domain (R836H and T844M), which constitutively activate Jak/Stat signaling [59-62], were observed only in early-onset precursor B-cell lymphomas (100% of cases) with high variant allele frequency (25–89%) (Figs. 8 and 9A). Likewise, mutations in *Jak1* within the pseudokinase domain

(H627Y and R723C/H), which may cooperatively activate the Jak/Stat pathway in *Jak3* mutants [63], were also observed in half of the early-onset precursor B-cell lymphomas (Figs. 8 and 9B). In addition, copy-number loss of *Pax5* was found at high frequency only in the early-onset precursor B-cell lymphomas (5/6 cases: 83%). The frequent aberrations in *Jak1/3* and *Pax5* were confirmed using an additional three early-onset precursor B-cell lymphomas collected from irradiated mice during the previous study in NIRS, QST [22] (Table 5). On the other hand, genetic alterations in a variety of cancer driver genes were identified in the late-onset and spontaneous B-cell lymphomas, whereas few alterations in these genes were found in the early-onset precursor B-cell lymphomas (Fig. 8). Among them, mutations in *Pim1* were the most frequently observed in some of the late-onset and spontaneous B-cell lymphomas. These data suggested that early-onset precursor B-cell lymphomas induced by radiation exposure harbor genomic alterations (i.e., mutation of *Jak3* and copy-number loss of *Pax5*) that are distinct from those of the other B-cell lymphomas.

2.3.2 Interstitial chromosomal deletion of *Pax5* in radiation-induced early-onset precursor B-cell lymphomas

Pax5, which encodes a transcription factor, is essential for commitment of lymphoid progenitors to the B lymphocyte lineage [20]. To further characterize the copy-number loss of *Pax5*, array-CGH analysis was performed on the early-onset precursor B-cell lymphomas. Consistent with the whole-exome sequencing data, partial copy-number losses of chromosome 4 region (i.e., interstitial chromosomal deletion), including the *Pax5* locus, were observed in five of six early-onset precursor B-cell lymphomas (cases 5, 7, 11, 14, and 19) (Fig. 10A). The entire *Pax5* allele was lost in three of these B-cell

lymphomas (cases 7, 11 and 19) (Fig. 10B). Homozygous deletion of exon 6 in *Pax5* was found in one B-cell lymphoma (case 19), resulting in the complete loss of Pax5 function. Partial hemizygous deletions of *Pax5* were also observed in the remaining two B-cell lymphomas (cases 5 and 14). These observations suggested that radiation-induced dysfunction of *Pax5* plays an important role in the development of early-onset precursor B-cell lymphomas.

2.3.3 Impact of *Pax5* genomic alteration in radiation-induced early-onset precursor B-cell lymphomas

To investigate the impact of *Pax5* genomic alteration in the early-onset precursor B-cell lymphomas, the expression of *Pax5* gene and its major transactivating target genes *Blnk* and *Cd19* [20] in the B-cell lymphomas was examined (Fig. 11). Consistent with the array-CGH data, *Pax5* expression was very low in two early-onset precursor B-cell lymphomas (cases 7 and 19) (Fig. 11A). Unexpectedly, *Pax5* expression was upregulated in the remaining four early-onset precursor B-cell lymphomas (cases 5, 11, 12 and 14), indicating the existence of positive feedback mechanisms. Moreover, immunostaining revealed the absence of cellular Pax5 in two early-onset precursor B-cell lymphomas (cases 7 and 19) (Fig. 11B), suggesting the involvement of epigenetic silencing (case 7) and homozygous deletion (case 19) of *Pax5*. Consistent with this observation, both *Blnk* and *Cd19* were downregulated in two other early-onset precursor B-cell lymphomas (cases 7 and 19) (Fig. 11C). On the other hand, *Blnk* and *Cd19* were upregulated in the remaining four B-cell lymphomas in which *Pax5* expression was elevated (cases 5, 11, 12 and 14).

PAX5 is a haploinsufficient tumor-suppressor gene in human B-ALL via its aberrant induction of its target genes [64, 65]. Thus, to gain a better understanding of how *Pax5* deletion affects the development of precursor B-cell lymphomas after radiation exposure, RNA-seq data of early-onset B-cell lymphomas were compared with those of late-onset precursor B-cell lymphomas. As shown in Fig. 12A, RNA-seq analysis identified 247 differentially expressed genes (≥2-fold change, $P < 0.05$), among which 128 were upregulated and 119 downregulated in the early-onset precursor B-cell lymphomas compared with late-onset precursor B-cell lymphomas. Gene Ontology analysis indicated that the differentially expressed genes were mostly enriched in B cell–related immune responses, i.e., activation, proliferation and differentiation of lymphocytes (Table 6), suggesting phenotypic differences between the early-onset and late-onset precursor B-cell lymphomas. Notably, hierarchical clustering of the differentially expressed genes allowed for the separation of the early-onset precursor B-cell lymphomas into $Pax5^{-}$ (cases 7 and 19) and $Pax5^{+}$ (cases 5, 11, 12 and 14) groups (Fig. 12A), which may reflect the ability of *Pax5* to be transcribed. Using the RNA-seq data, the gene set enrichment analysis (GSEA) was preformed to examine whether the $Pax5^{+}$ early-onset and late-onset B-cell lymphomas have a phenotype of precursor B cells. This revealed that the gene-expression profile of early-onset precursor B-cell lymphomas correlated positively with that of precursor B cells and negatively with mature B cells, as reported previously [66] (Fig. 12B and C and Table 7). As expected, genes involved in precursor B-cell survival (e.g., *Igll1*, *Xrcc6*, *Rag1/2*, *Sox4*, *Il7r*) [67-69] were upregulated in the early-onset precursor B-cell lymphomas compared with the late-onset precursor B-cell lymphomas (Fig. 12D and E). In addition, certain known *Pax5*-repressed genes, including *Ramp1*, *Tnfsf11*, *Vav3*, *Satb1*, *Emb*, *Notch1* and *Flt3* [20], were upregulated in the early-onset

precursor B-cell lymphomas compared with the late-onset precursor B-cell lymphomas (Fig. 13), indicating a dysfunction of *Pax5* in the early-onset precursor B-cell lymphomas. These data suggested that, although radiation-induced early-onset precursor B-cell lymphomas can be subdivided into $Pax5^{-}$ and $Pax5^{+}$ cases, those B-cell lymphomas have the gene-expression profile of B-ALL with dysregulation of the *Pax5*-targeted genes. On the other hand, expression profiles for late-onset precursor B-cell lymphomas correlated with a variety of gene-expression signatures from hematopoietic cells other than precursor B cells (Table 8), suggesting that late-onset precursor B-cell lymphomas are composed of heterogenous subsets with diverse phenotypes.

2.3.4 Identification of fusion genes in radiation-induced early-onset precursor B-cell lymphomas

Because oncogenic fusion genes are involved in human ALL with *Pax5* deletion [70], the expression of fusion transcripts in the early-onset precursor B-cell lymphomas was analyzed using RNA-seq data. Multiple fusion transcripts were identified in the early-onset precursor B-cell lymphomas (Fig. 14). However, none of the early-onset precursor B-cell lymphomas expressed the oncogenic fusion genes found in approximately half of human ALLs (*BCR-ABL1*, *TCF3-PBX1*, *ETV6-RUNX1*, and various fusions involving *KMT2A* and *CRLF2*) [18]. These data suggested that the oncogenic fusion genes that commonly drive human ALL are not involved in the development of early-onset precursor B-cell lymphoma after radiation exposure.

Activation of Jak/Stat signaling in radiation-induced early-onset precursor B-cell lymphomas

All the early-onset precursor B-cell lymphomas had missense mutations in the kinase domain of *Jak3* (Fig. 8), and this was confirmed by sequencing of the corresponding cDNAs (Fig. 15). Notably, mouse Jak3 mutants R653H and V670A and their human orthologs are known to phosphorylate Stat5, leading to the progression of ALL [59, 63]. Therefore, the phosphorylation status of Stat5 in B-cell lymphomas was analyzed using western capillary electrophoresis. As expected, Stat5 phosphorylation was elevated in all the early-onset precursor B-cell lymphomas compared with the other B-cell lymphomas (Fig. 16). These results suggested that activation of Jak3/Stat5 signaling is critical for early induction of precursor B-cell lymphomas after radiation exposure.

Table 5. Aberrations of human ALL-related genes identified in early-onset lymphomas developed in mice irradiated with 3.8 Gy of X-rays

Case no.	Lifespan (weeks)	Gene	Mutation (VAF)	CNA
X1	27	*Jak3*	R653H (85 %)	ND
		Jak1	R723C (19 %)	ND
		Pax5	ND	Loss
X3	30	*Jak3*	R653H (47 %)	ND
X4	35	*Jak3*	R653H (23 %)	ND
		Stat5a	P693S (14 %)	ND
		Pax5	ND	Loss

VAF, variant allele frequency; CNA, copy number alteration; ND, not detected.

Table 6. Top 50 of gene ontology (GO) terms enriched with differentially expressed genes between early-onset and late-onset B-cell lymphomas

Ontology	GO Term	GO ACCESSION	Corrected *P*-value	Count in selection
Biological Process	lymphocyte activation	GO:0046649	0.0000	15
Biological Process	leukocyte activation	GO:0045321	0.0000	16
Biological Process	cell activation	GO:0001775	0.0000	17
Biological Process	establishment of endothelial barrier	GO:0061028	0.0001	4
Biological Process	regulation of signal transduction	GO:0009966|GO:0035466	0.0001	41
Biological Process	lymphocyte proliferation	GO:0046651	0.0001	6
Biological Process	mononuclear cell proliferation	GO:0032943	0.0001	6
Biological Process	regulation of signaling	GO:0023051	0.0001	44
Biological Process	regulation of GTPase activity	GO:0043087|GO:0032312|GO:0032313|GO:0032314|GO:0032315|GO:0032316|GO:0032317|GO:0032318|GO:0032319|GO:0043088	0.0001	12
Biological Process	regulation of hydrolase activity	GO:0051336	0.0002	22
Biological Process	leukocyte proliferation	GO:0070661	0.0002	6
Biological Process	regulation of response to stimulus	GO:0048583	0.0002	48
Biological Process	B cell activation	GO:0042113	0.0002	7
Biological Process	regulation of cell communication	GO:0010646	0.0002	43
Biological Process	endothelial cell differentiation	GO:0045446	0.0002	5
Biological Process	anatomical structure morphogenesis	GO:0009653	0.0003	31
Biological Process	lymphocyte activation involved in immune response	GO:0002285	0.0003	6
Biological Process	B cell activation involved in immune response	GO:0002312	0.0003	4
Biological Process	regulation of cellular component size	GO:0032535	0.0004	10
Biological Process	negative regulation of I-kappaB kinase/NF-kappaB signaling	GO:0043124	0.0004	4
Biological Process	regulation of anatomical structure size	GO:0090066	0.0004	12
Biological Process	endothelial cell development	GO:0001885	0.0005	4
Biological Process	endothelium development	GO:0003158	0.0005	5
Biological Process	negative regulation of NIK/NF-kappaB signaling	GO:1901223|GO:0042347	0.0006	3
Biological Process	regulation of actin filament organization	GO:0110053	0.0006	8

Table 6. Top 50 of gene ontology (GO) terms enriched with differentially expressed genes between early-onset and late-onset B-cell lymphomas (continued)

Ontology	GO Term	GO ACCESSION	Corrected *P*-value	Count in selection
Biological Process	B cell proliferation involved in immune response	GO:0002322	0.0007	2
Biological Process	negative regulation of interferon-alpha production	GO:0032687|GO:0045355|GO:1902740	0.0007	2
Biological Process	signal transduction in response to DNA damage	GO:0042770	0.0007	4
Biological Process	T cell activation	GO:0042110	0.0008	8
Biological Process	developmental process	GO:0032502|GO:0044767	0.0008	62
Biological Process	activated T cell proliferation	GO:0050798	0.0010	2
Biological Process	regulation of interferon-alpha production	GO:0032647|GO:0045354|GO:1902739	0.0012	3
Biological Process	cell differentiation	GO:0030154	0.0013	43
Biological Process	anatomical structure development	GO:0048856	0.0014	57
Biological Process	positive regulation of cell communication	GO:0010647	0.0014	24
Biological Process	positive regulation of signal transduction	GO:0009967|GO:0035468	0.0014	22
Biological Process	positive regulation of signaling	GO:0023056	0.0015	24
Biological Process	leukocyte activation involved in immune response	GO:0002366	0.0015	6
Biological Process	cell activation involved in immune response	GO:0002263	0.0017	6
Biological Process	regulation of actin polymerization or depolymerization	GO:0008064	0.0018	6
Biological Process	cellular developmental process	GO:0048869	0.0018	43
Biological Process	regulation of actin filament length	GO:0030832	0.0018	6
Biological Process	regulation of toll-like receptor 9 signaling pathway	GO:0034163	0.0018	2
Biological Process	skeletal system morphogenesis	GO:0048705	0.0022	7
Biological Process	embryonic axis specification	GO:0000578	0.0023	3
Biological Process	establishment of endothelial intestinal barrier	GO:0090557	0.0023	2
Biological Process	regulation of cell-cell adhesion mediated by integrin	GO:0033632	0.0023	2
Biological Process	regulation of catalytic activity	GO:0050790|GO:0048552	0.0024	29
Biological Process	regulation of protein-containing complex assembly	GO:0043254	0.0024	9

Table 7. Gene sets significantly enriched in the early-onset B-cell lymphomas

Gene set name	NES	*P*-value	FDR *q*-value
MORI_MATURE_B_LYMPHOCYTE_DN	2.3	0.00	0.0
MORI_EMU_MYC_LYMPHOMA_BY_ONSET_TIME_UP	2.2	0.00	0.0
MORI_IMMATURE_B_LYMPHOCYTE_DN	2.1	0.00	0.0
MORI_LARGE_PRE_BII_LYMPHOCYTE_UP	1.9	0.00	0.1

FDR, false discovery rate; NES, normalized enrichment score.

Table 8. Gene sets significantly enriched in the late-onset B-cell lymphomas

Gene set name	NES	*P*-value	FDR *q*-value
CHYLA_CBFA2T3_TARGETS_DN	2.0	0.00	0.0
WP_CELL_DIFFERENTIATION_INDEX	1.9	0.00	0.0
WP_MIRNAS_INVOLVEMENT_IN_THE_IMMUNE_RESPONSE_IN_SEPSIS	1.8	0.00	0.1
REACTOME_FORMATION_OF_FIBRIN_CLOT_CLOTTING_CASCADE	1.8	0.00	0.1
REACTOME_COPI_MEDIATED_ANTEROGRADE_TRANSPORT	1.8	0.00	0.1
WELCH_GATA1_TARGETS	1.8	0.00	0.1
KEGG_ALLOGRAFT_REJECTION	1.8	0.00	0.1
WP_BLOOD_CLOTTING_CASCADE	1.8	0.00	0.1
DAVIES_MULTIPLE_MYELOMA_VS_MGUS_DN	1.8	0.00	0.1
WP_CELL_DIFFERENTIATION_INDEX_EXPANDED	1.7	0.00	0.1
REACTOME_DEFECTS_OF_CONTACT_ACTIVATION_SYSTEM_CAS_AND_KALLIKREIN_KININ_SYSTEM_KKS	1.7	0.00	0.1
KEGG_TYPE_I_DIABETES_MELLITUS	1.7	0.00	0.1
REACTOME_BETA_DEFENSINS	1.7	0.00	0.2
WP_FOLATE_METABOLISM	1.7	0.00	0.2
KEGG_LEISHMANIA_INFECTION	1.7	0.00	0.2
ALTEMEIER_RESPONSE_TO_LPS_WITH_MECHANICAL_VENTILATION	1.7	0.00	0.2
KEGG_AUTOIMMUNE_THYROID_DISEASE	1.7	0.00	0.2
REACTOME_PLATELET_ADHESION_TO_EXPOSED_COLLAGEN	1.7	0.00	0.2
WP_INTRACELLULAR_TRAFFICKING_PROTEINS_INVOLVED_IN_CMT_NEUROPATHY	1.7	0.00	0.2
WP_WNT_SIGNALING_IN_KIDNEY_DISEASE	1.7	0.00	0.2
ICHIBA_GRAFT_VERSUS_HOST_DISEASE_35D_UP	1.7	0.00	0.2
JAATINEN_HEMATOPOIETIC_STEM_CELL_DN	1.7	0.00	0.2

Table 8. Gene sets significantly enriched in the late-onset B-cell lymphomas (continued)

LINDSTEDT_DENDRITIC_CELL_MATURATION_B	1.7	0.00	0.2
LIAN_LIPA_TARGETS_3M	1.7	0.00	0.2
WP_ALLOGRAFT_REJECTION	1.7	0.00	0.2
WP_VITAMIN_B12_METABOLISM	1.7	0.00	0.2
SHIN_B_CELL_LYMPHOMA_CLUSTER_9	1.7	0.00	0.2
VALK_AML_CLUSTER_7	1.7	0.01	0.2
LIAN_NEUTROPHIL_GRANULE_CONSTITUENTS	1.7	0.00	0.2
REACTOME_ER_TO_GOLGI_ANTEROGRADE_TRANSPORT	1.7	0.00	0.2
BOYLAN_MULTIPLE_MYELOMA_C_D_DN	1.7	0.00	0.2
VERHAAK_AML_WITH_NPM1_MUTATED_UP	1.7	0.00	0.2
BASSO_CD40_SIGNALING_UP	1.7	0.00	0.2
REACTOME_METABOLIC_DISORDERS_OF_BIOLOGICAL_OXIDATION_ENZYMES	1.6	0.00	0.2
RHEIN_ALL_GLUCOCORTICOID_THERAPY_UP	1.6	0.01	0.2
KLEIN_PRIMARY_EFFUSION_LYMPHOMA_DN	1.6	0.00	0.2
GAURNIER_PSMD4_TARGETS	1.6	0.00	0.2
CHEOK_RESPONSE_TO_MERCAPTOPURINE_AND_LD_MTX_DN	1.6	0.00	0.2
REACTOME_ROS_AND_RNS_PRODUCTION_IN_PHAGOCYTES	1.6	0.01	0.2
REACTOME_INTRINSIC_PATHWAY_OF_FIBRIN_CLOT_FORMATION	1.6	0.01	0.2
WP_IL1_AND_MEGAKARYOCYTES_IN_OBESITY	1.6	0.01	0.2
REACTOME_BMAL1_CLOCK_NPAS2_ACTIVATES_CIRCADIAN_GENE_EXPRESSION	1.6	0.01	0.2
KEGG_GRAFT_VERSUS_HOST_DISEASE	1.6	0.00	0.2

FDR, false discovery rate; NES, normalized enrichment score.

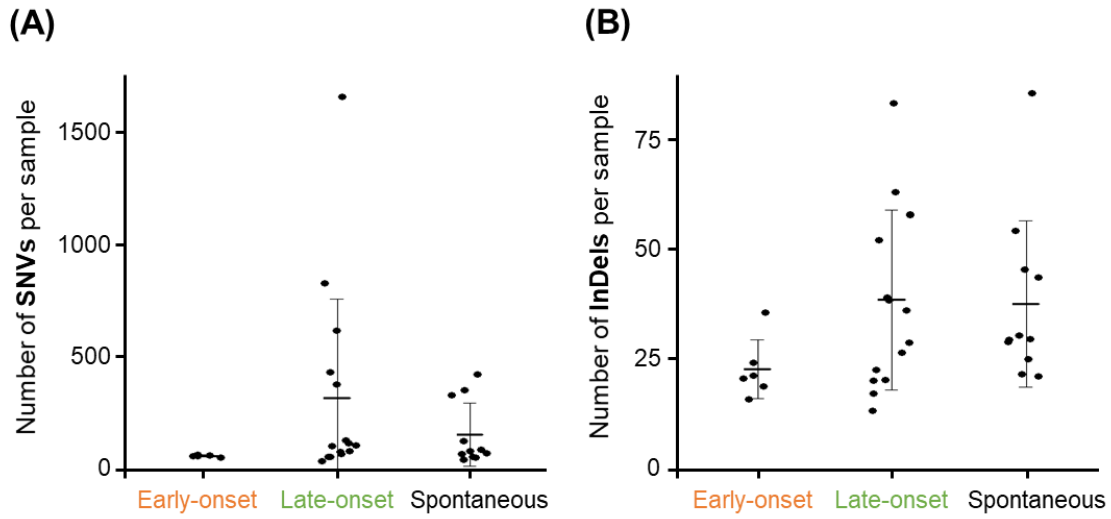

Figure 7. Number of somatic mutations identified in B-cell lymphomas. The number of (**A**) single nucleotide variants (SNVs) and (**B**) insertions and deletions (InDels) found in the early-onset B-cell lymphomas (n = 6), late-onset B-cell lymphomas (n = 15), and spontaneous B-cell lymphomas (n = 11). The data represent the mean ± SD. No significant differences were observed with respect to the number of SNVs and InDels among the three types of B-cell lymphomas.

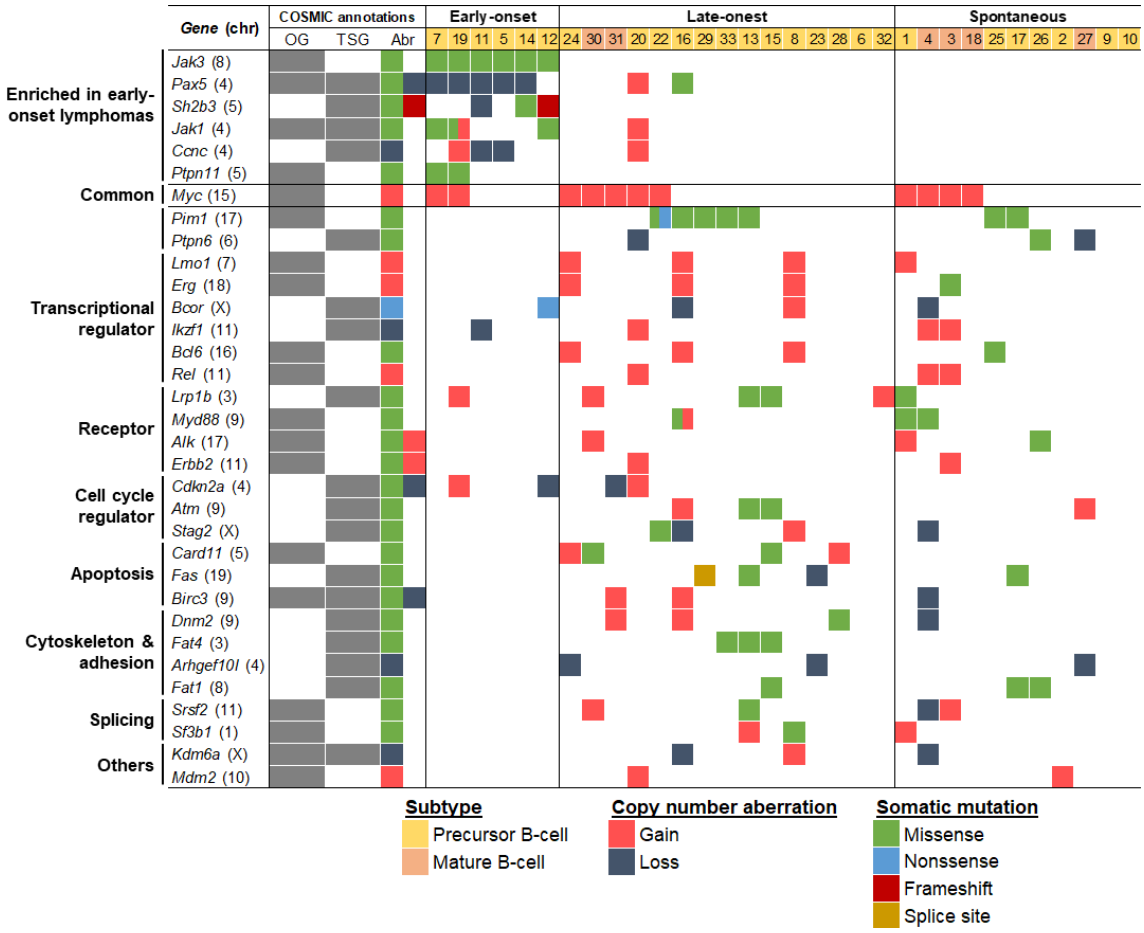

Figure 8. Candidate driver genes of B-cell lymphomas in mice. Human hematopoietic neoplasm–related cancer genes with somatic mutations and/or copy-number alternations found in early-onset B-cell lymphomas (n = 6) and late-onset B-cell lymphomas (n = 15) from irradiated mice and spontaneous B-cell lymphomas (n = 11). The genes were considered as responsible if their aberrations matched those registered in the Catalogue of Somatic Mutations in the Cancer Gene Census database and not registered as mouse single nucleotide polymorphisms in the SNP database. Numbers across the top indicate case numbers. Chr, chromosome number; OG, oncogene; TSG, tumor-suppressor gene; Abr, aberrations.

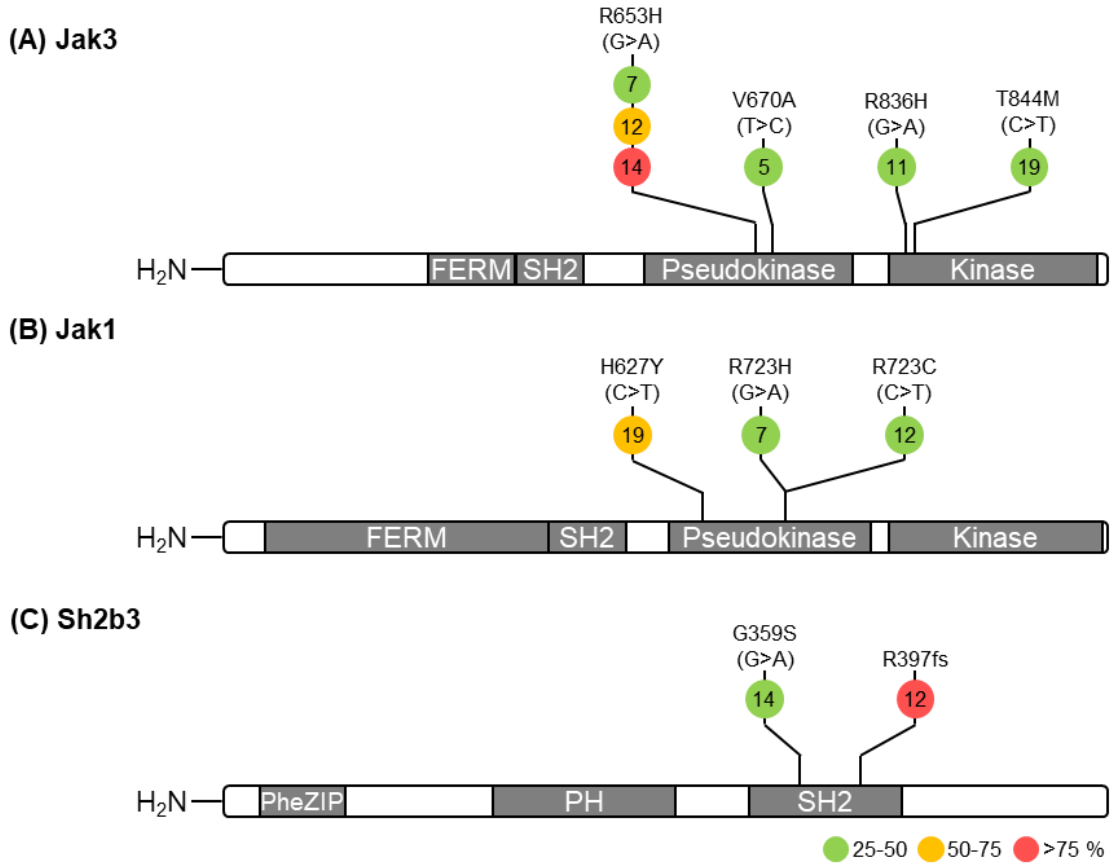

Figure 9. Schematics for the proteins (A) Jak3, (B) Jak1 and (C) Sh2b3. Showing the positions of individual somatic mutations identified in the B-cell lymphomas. Numbers in circles indicate case numbers, and the colors denote variant allele frequency of the mutations per the color key shown at the bottom.

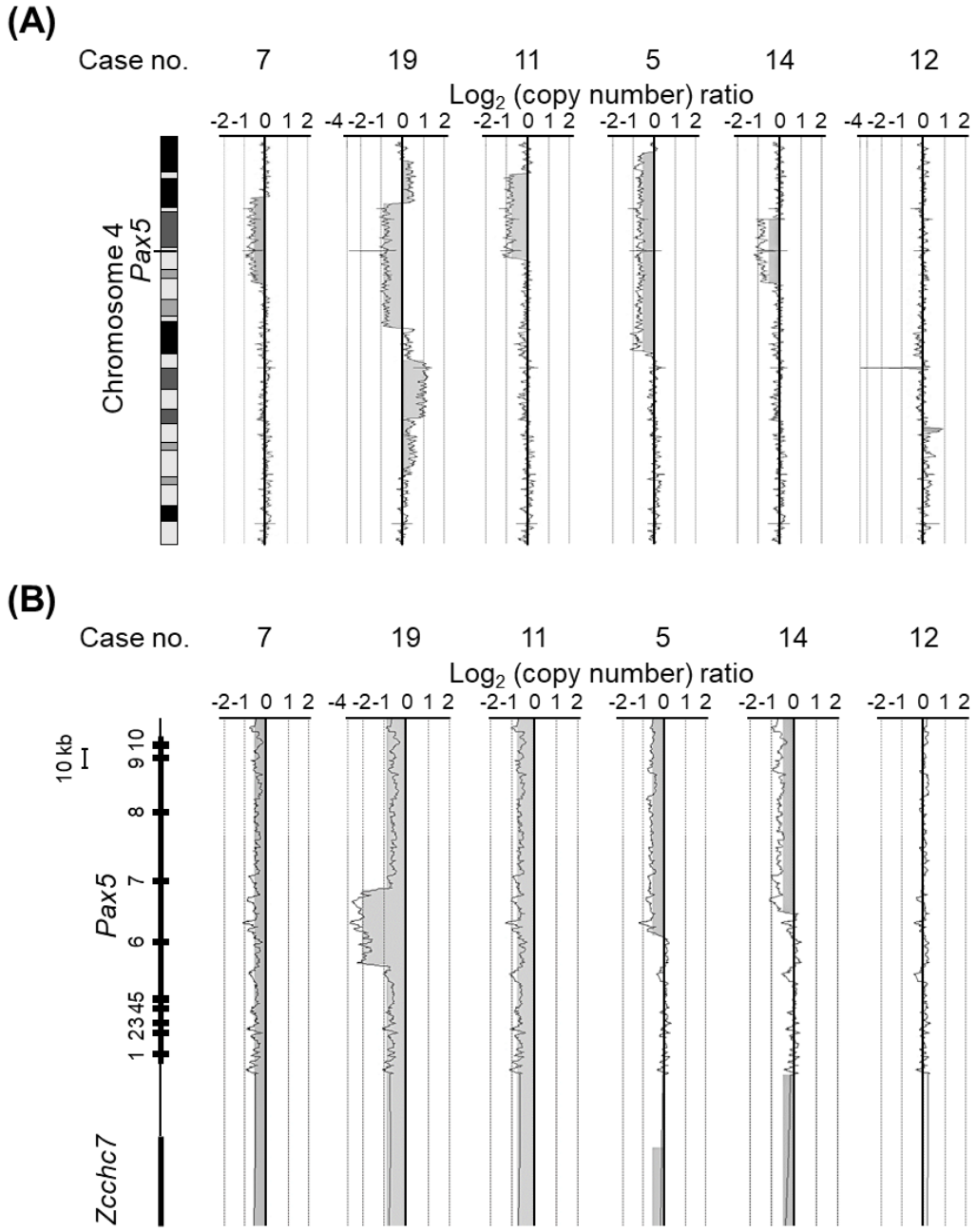

Figure 10. Copy number changes on chromosome 4 in radiation-induced early-onset precursor B-cell lymphomas. Copy-number alterations on (**A**) whole chromosome 4 and (**B**) the *Pax5 locus* (4qB1) in the early-onset precursor B-cell lymphomas (n = 6) were analyzed by array-CGH. The *x* axis shows the log2 ratio value for each B-cell lymphoma (tumor genomic DNA versus normal control genomic DNA). The regions with copy-number alterations are shaded in gray.

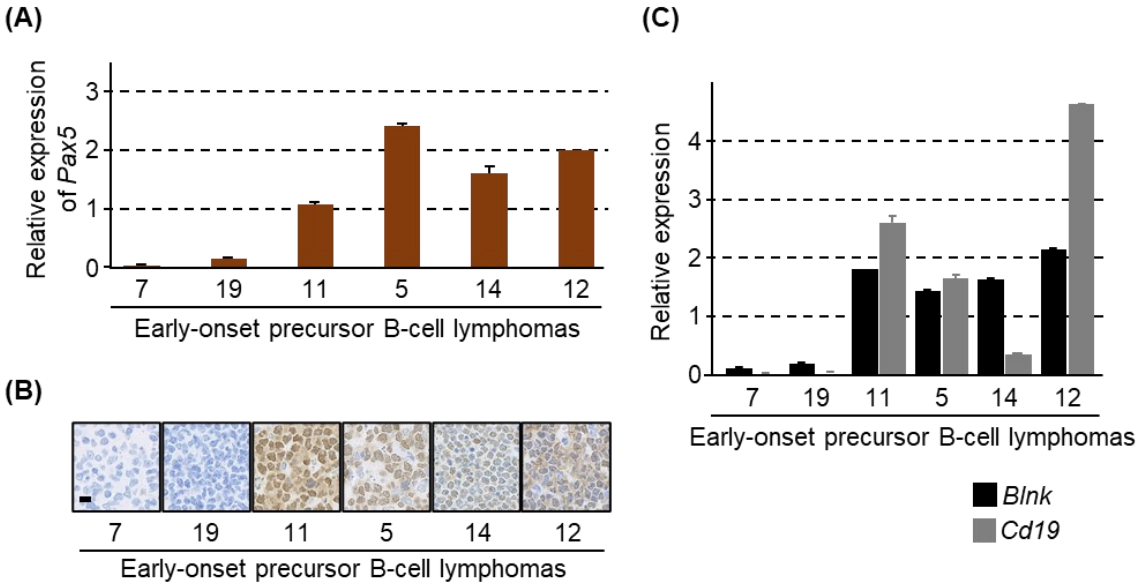

Figure 11. Changes in the expression of *Pax5* and its target genes in radiation-induced early-onset precursor B-cell lymphomas. (**A**) Relative expression of *Pax5* in early-onset precursor B-cell lymphomas analyzed by quantitative reverse transcription-PCR. The expression of *Gapdh* was used as the internal control. The data were normalized such that the mean expression levels for spontaneous B-cell lymphomas equaled 1. Data represent the mean ± SD of at least two independent experiments. (**B**) Immunohistochemical staining for Pax5 in early-onset precursor B-cell lymphomas. All images were acquired at the same magnification. Scale bar, 10 μm. (**C**) Relative expression of *Blnk* and *Cd19* in early-onset precursor B-cell lymphomas analyzed by quantitative reverse transcription-PCR. Data were normalized as above.

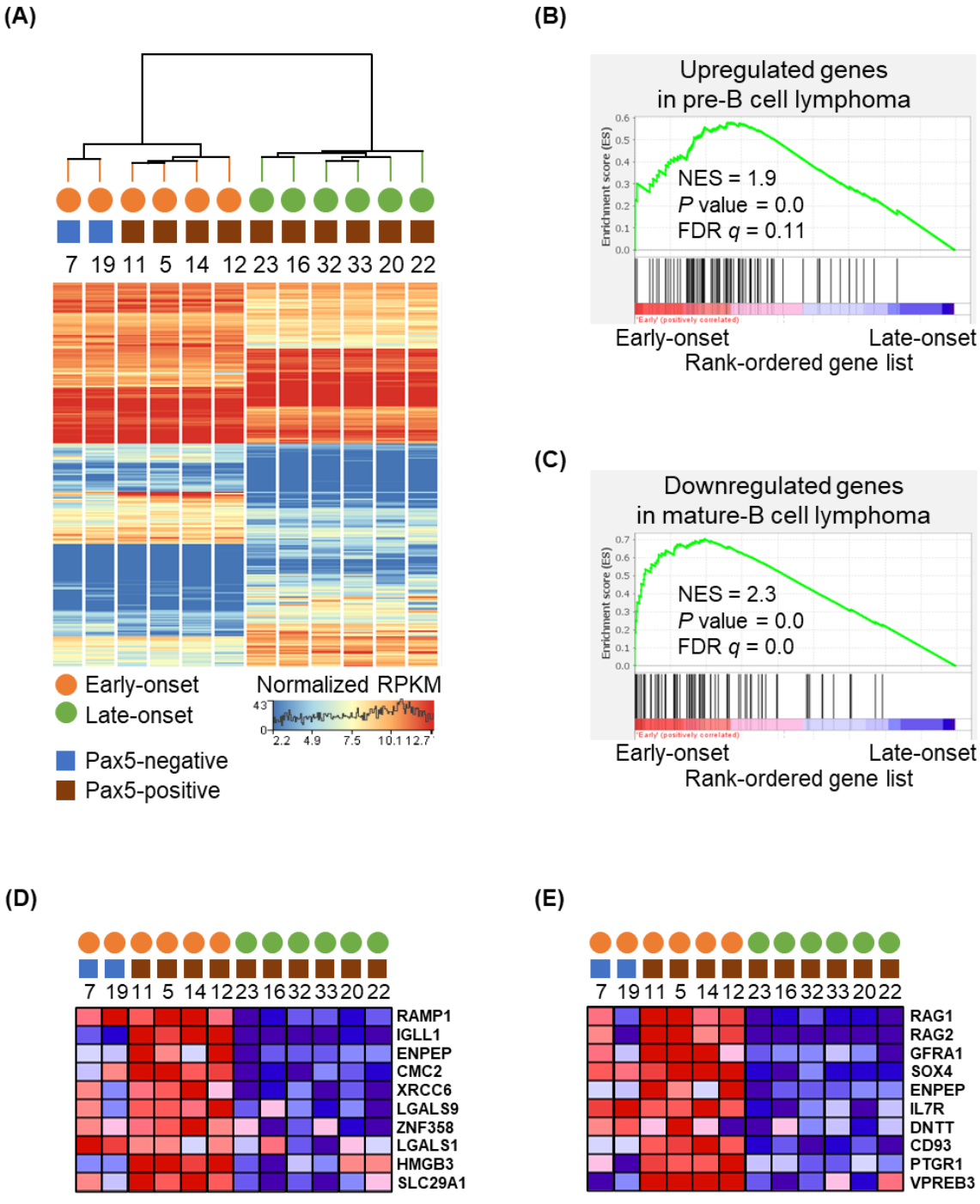

Figure 12. RNA-seq of precursor B-cell lymphomas of irradiated mice. The legends are shown on the next page.

(**A**) Hierarchical clustering of differentially expressed genes between early-onset precursor B-cell lymphomas (n = 6) and late-onset precursor B-cell lymphomas (n = 6). The three colors (red, pink, blue) correspond to the range of expression values (high, moderate, low). (**B** and **C**) GSEA plot showing the enrichment of a set of upregulated genes in precursor B-cell lymphomas (MORI_LARGE_PRE_BII_LYMPHOCYTE_UP) [66] (B) and a set of down-regulated genes in mature B-cell lymphoma (MORI_MATURE_B_LYMPHOCYTE_DN) (C) among the early-onset precursor B-cell lymphomas. FDR, false discovery rate; NES, normalized enrichment score. Color ranges from dark red to dark blue represents the highest and lowest expression of a gene, respectively. (**D** and **E**) Heat map of the top 10 upregulated genes in the early-onset precursor B-cell lymphomas in the gene sets of the upregulated genes in precursor B-cell lymphomas (D) and the down-regulated genes in mature B-cell lymphoma (E).

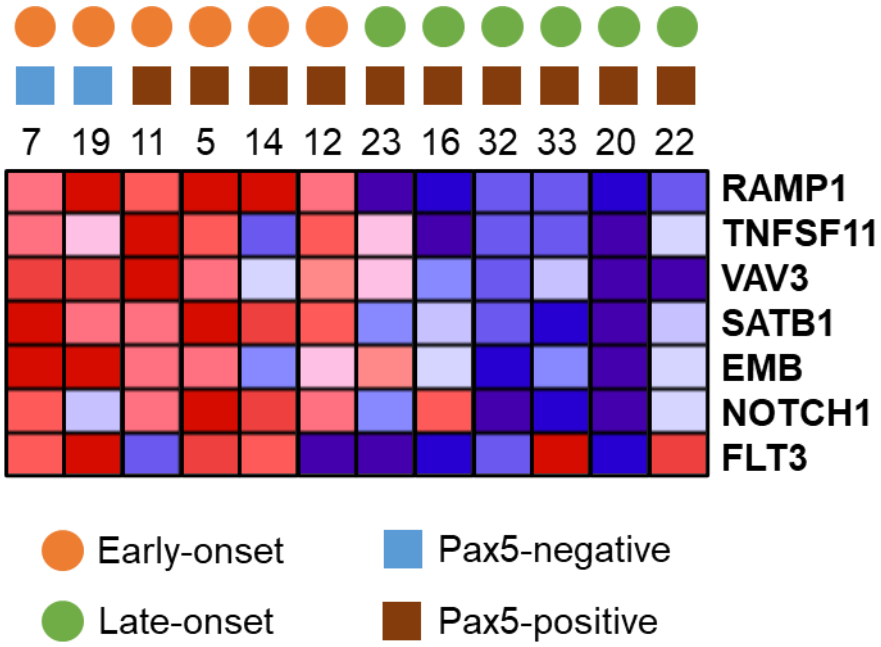

Figure 13. Upregulation of Pax5-repressed genes in radiation-induced early-onset precursor B-cell lymphomas. Heat map of known Pax5-repressed genes expressed in early- and late-onset precursor B-cell lymphomas.

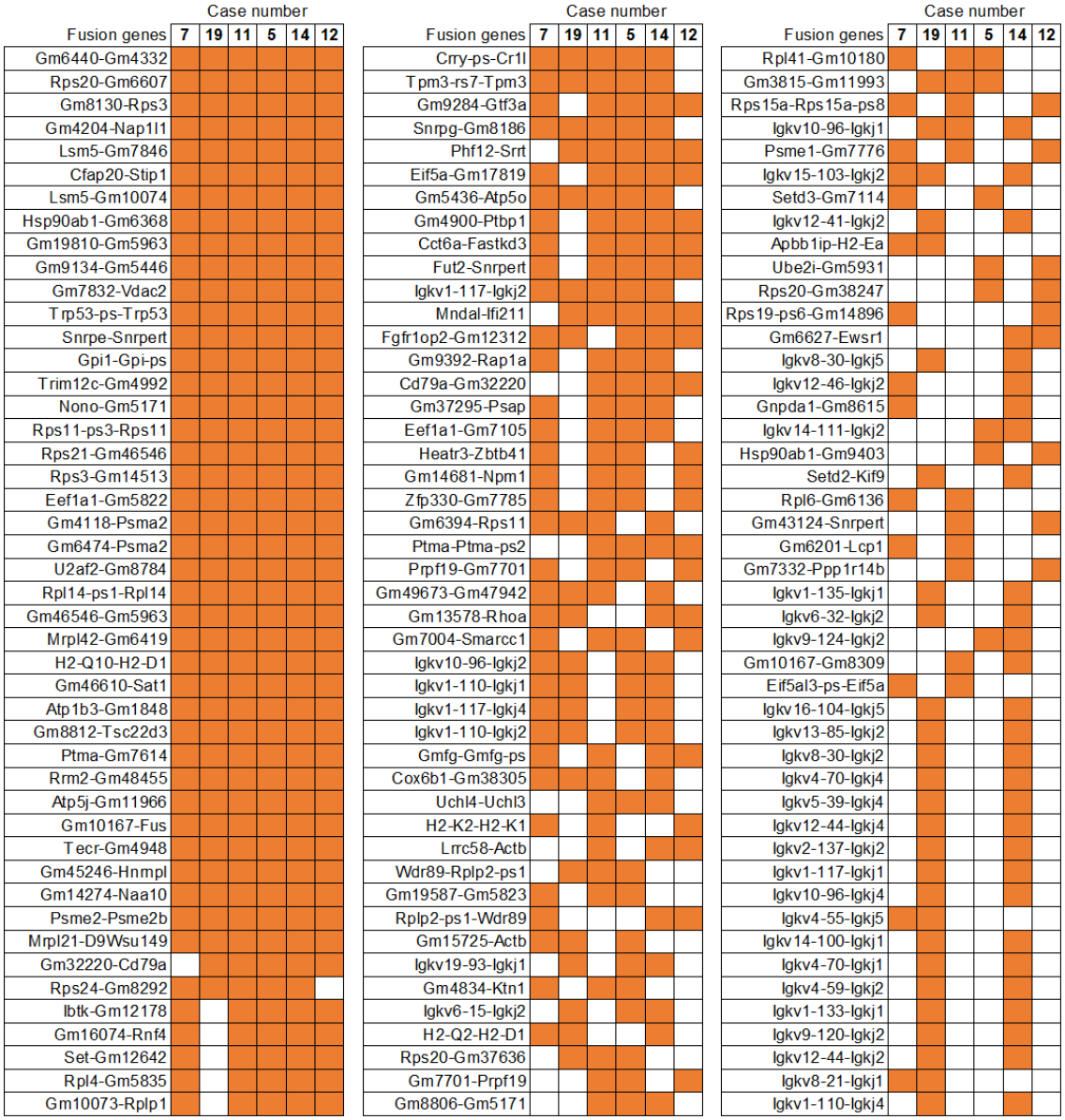

Figure 14. Fusion transcripts detected in the early-onset precursor B-cell lymphomas. Fusion transcripts with more than 10 junction reads that detected in at least two early-onset lymphomas are shown. Orange columns indicate the expression of fusion transcripts.

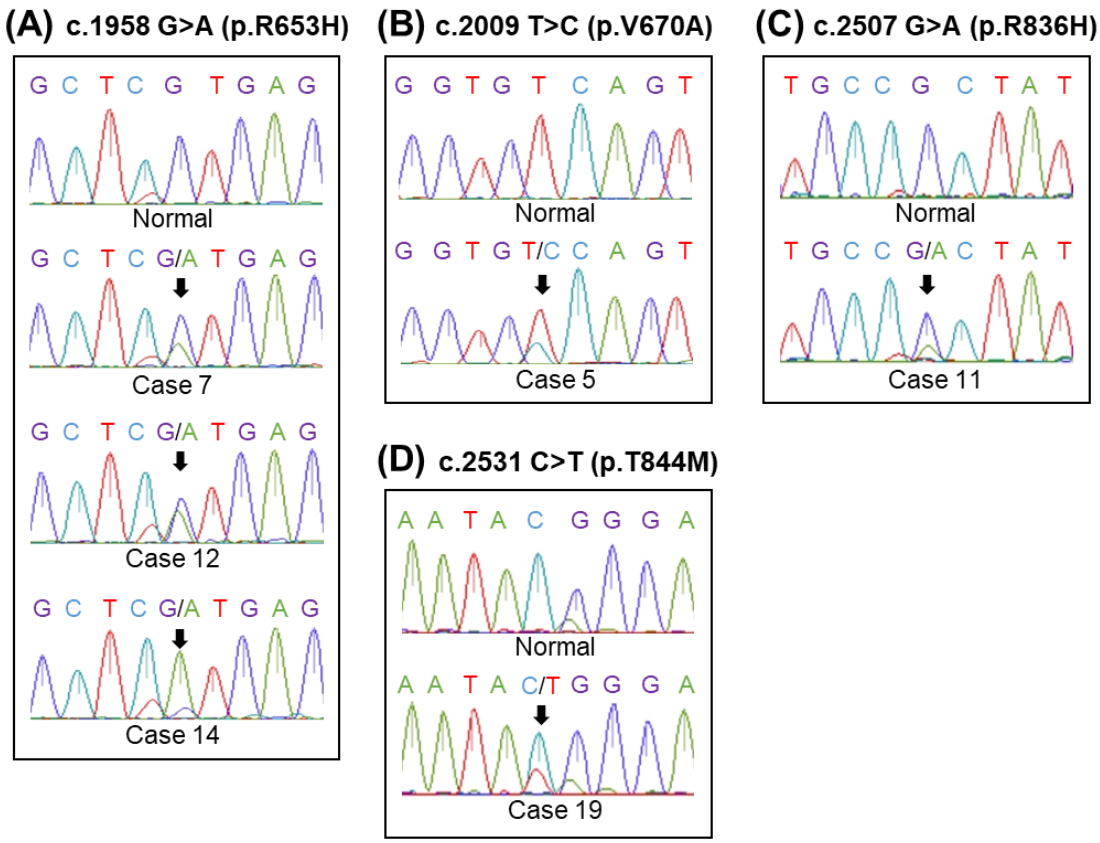

Figure 15. Validation of expression the mutant Jak3 expression in the early-onset precursor B-cell lymphomas. Mutant Jak3 transcripts of (**A**) R653H, (**B**) V670A, (**C**) R836H and (**D**) T844M were analyzed by Sanger sequencing. Data for a B-cell lymphoma (case number 3) represent a normal sample, i.e., without *Jak3* mutation.

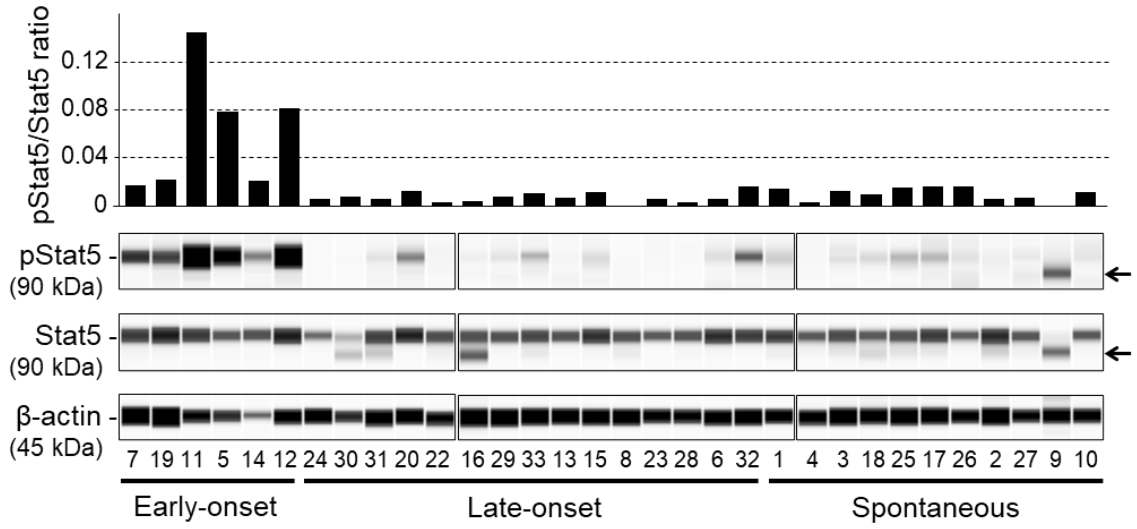

Figure 16. Activation of Jak/Stat signaling pathway in radiation-induced early-onset precursor B-cell lymphomas. Expression of phospho-Stat5 (pStat5) and Stat5 proteins in the B-cell lymphomas was analyzed by western capillary electrophoresis. Arrows indicate the short form (~75 kDa) of Stat5, possibly generated by the cathepsin G–mediated proteolysis of full-length Stat5 (90 kDa) during the protein extraction procedure [71]. β-actin was used as the loading control. The ratio between the area under curve for each of full-length Stat5 and pStat5 was calculated as the pStat5/Stat5 ratio for each sample.

2.4 Discussion

In the present study, whole-exome sequencing of mice B-cell lymphomas identified frequent copy-number losses of *Pax5* and gain-of-function mutations of *Jak3* in early-onset precursor B-cell lymphomas that developed after radiation exposure (Fig. 8 and Table 5). Interestingly, these aberrations also have been observed in a subset of human B-ALLs, including Ph-like ALL [72-76], which is a recently described ALL subset characterized by diverse genetic alterations that result in the dysregulation of cytokine-receptor and kinase signaling. Despite the lack of fusion genes (e.g., *BCR-ABL1*), the characteristics of Ph-like ALL, which is associated with poor outcome after conventional therapeutic approaches, are quite similar to these of Ph-positive ALL [76]. Consistent with this, negative expression of oncogenic fusion genes, i.e., *BCR-ABL1*, *ETV6-RUNX1*, *TCF3-PBX1* and various *KMT2A* fusions, was observed in all early-onset B-cell lymphoma cases (Fig. 14). In addition, deletion of *Ikzf1* and loss-of-function mutations of *Sh2b3*, which are also reported as genetic features of the Ph-like ALL [50, 73], were found in some of the early-onset precursor B-cell lymphomas (Fig. 8). These results suggest that genetic features of radiation-induced early-onset precursor B-cell lymphoma are similar to those of human Ph-like ALL. On the other hand, genetic alterations in *Pim1*, *Fat4*, *Myd88* and *Card11* genes were identified in some of the late-onset and spontaneous B-cell lymphomas (Fig. 8). Mutations of these genes occur frequently in human diffuse large lymphoma [77], suggesting that a subset of the late-onset and spontaneous B-cell lymphomas harbor genetic aberrations similar to those of diffuse large B-cell lymphoma.

Ionizing radiation induces DNA double-strand breaks that can lead to chromosomal deletions. Indeed, interstitial chromosomal deletions of specific tumor-suppressor genes have been reported in several radiation-induced rodent models of

cancers, including acute myeloid leukemia (*Sfpi1*), medulloblastoma (*Ptch1*), and renal tumor (*Tsc2*) [78-81]. Consistent with these findings, the present study revealed frequent interstitial chromosomal deletions of the tumor-suppressor gene *Pax5*, i.e., in five of six radiation-induced early-onset precursor B-cell lymphomas (Fig. 10A). However, *Pax5* was downregulated in two of six early-onset precursor B-cell lymphomas, whereas it was upregulated in other cases (Fig. 11A). In this regard, transcriptional activation of *Pax5* by Stat5, a downstream transcription factor of the Jak/Stat signaling pathway, has been reported as a positive feedback mechanism [82]. Therefore, despite the deletion of *Pax5* in the majority of early-onset precursor B-cell lymphomas, the upregulation of this gene in some of the early-onset precursor B-cell lymphomas may have been caused by mutant Jak3–induced activation of Stat5 (as shown in Fig. 16) during the process of carcinogenesis. This scenario is also supported by the fact that *PAX5* is highly expressed in ~90% of human B-ALL cases, including ALLs in which PAX5 is truncated [83].

Previous studies have demonstrated that precursor B cells, which depend on the Il-7/Jak3/Stat5 axis for their survival, are enriched in bone marrow of *Pax5* heterozygotes (mouse model) compared with wild-type mice [59, 84]. Notably, in this mouse model, B-ALL with *Jak3* mutation develops frequently after exposure to infection or a chemical mutagen but does not develop spontaneously [59, 84]. Likewise, hypersensitivity of pro-B cells to Il-7 and rapid induction of B-ALL have been reported in a mouse knockout model of *Sh2b3*, which encodes a Jak3 inhibitor [38, 85]. Consistent with these observations, in the present study, several genes that are needed for the survival of precursor B cells (e.g., *Il-7r*) were upregulated in early-onset precursor B-cell lymphomas compared with late-onset precursor B-cell lymphomas (Fig. 12E). In addition, the early-onset precursor B-cell lymphomas harbored mutations in three genes (*Jak3*, *Jak1*, *Sh2b3*)

related to the Jak/Stat pathway that had high variant allele frequencies (Fig. 9), suggesting that these mutations are present in the majority of malignant cells in B-cell lymphomas. Notably, almost all of the identified base-substitution mutations (8 of 10) in these genes were C:G>T:A transitions at CpG sites, which are attributed to spontaneous deamination of 5-methylcytosine [86]. These findings suggest that mutations in these genes are an early-onset event in radiation-induced lymphomagenesis, possibly occurring during the obligate cell proliferation associated with recovery from bone-marrow damage. Collectively, the data of the present study suggest that loss-of-function of *Pax5* or *Sh2b3* increases the population of Il-7-sensitive precursor B cells and that *Jak1/3* mutations are acquired during the proliferation of these precursor B cells after radiation exposure.

To further validate that *Pax5* is a driver gene of radiation-induced early-onset precursor B-cell lymphomas, an animal experiment was currently in progress using a *Pax5-floxed;Rosa26-CreER*^{T2} mice, in which conditional hemi-deletion of *Pax5* can be induced by tamoxifen injection (Fig. 17A). In this experiment, the mice were divided into five experimental groups as follows: 4 or 2 Gy of gamma-irradiated or non-irradiated groups after administration of tamoxifen and 4 Gy of gamma-irradiated or non-irradiated groups without tamoxifen administration (Fig. 17B). As shown in Fig. 18A, a dose-dependent induction of lymphomas was observed in irradiated *Pax5*$^{+/-}$ mice in observation until 45 weeks of age, while no lymphoma was observed in irradiated *Pax5* $^{+/+}$ mice and non-irradiated *Pax5* $^{+/-}$ mice. Notably, the majority of lymphomas were classified as the lymphomas other than thymic lymphoma (Non-TL), indicating the induction of B-cell lymphomas (Fig. 18B). These data suggest that *Pax5* is a driver gene of radiation-induced early-onset B-cell lymphomas and that additional carcinogenic events caused by radiation exposure are necessary for full malignancy of *Pax5* $^{+/-}$ pre-

lymphoma cells.

In conclusion, the present results demonstrate that loss of function of *Pax5* plays a critical role in initiating B-cell leukemogenesis and that cooperative activation of Jak3/Stat5 signaling leads to the rapid development of B-ALL following radiation exposure. In addition to these genetic alterations, the lack of oncogenic fusion genes in the B-cell lymphomas indicates that radiation-induced early-onset precursor B-cell lymphoma recapitulates features of Ph-like ALL. The findings provide new insights into the risk assessment of B-ALL after radiation exposure in the context of molecular signatures for radiation-induced cancers and molecular targeted therapy for B-ALL.

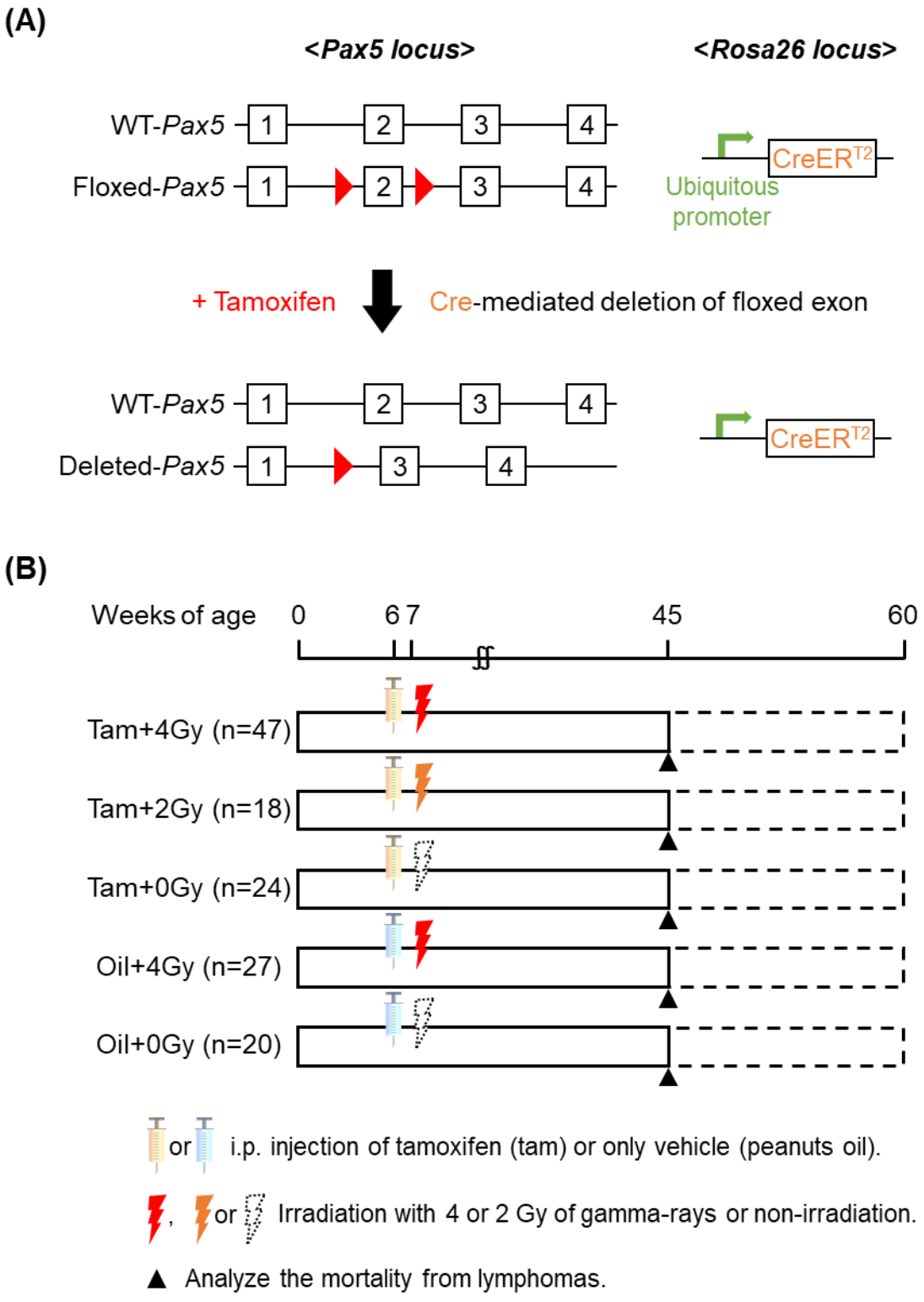

Figure 17. Experimental design using a *Pax5* conditional deletion mice. The legend is shown on the next page.

(**A**) *Pax5-floxed* male mice [87] and *Rosa26-CreER^{T2}* female mice [88] were purchased from Jackson Laboratory (Bar Harbor, ME) and then crossed to generate *Pax5$^{fl/+}$;Rosa26-CreER^{T2}* female and male mice, which carry a Cre-recombinase-Estrogen-Receptor-T2 allele in ubiquitously expressed *Rosa26 locus* and a floxed *Pax5* allele. In the absence of tamoxifen, Cre is expressed in cells of *Pax5$^{fl/+}$;Rosa26-CreER^{T2}* mice but Cre protein is not active. Upon tamoxifen-administration, however, Cre can mediate recombination of DNA sequence, including the exon 2 in one allele of *Pax5*, flanked by *loxP* sites (shown as triangles) resulting in hemi-deletion of *Pax5*. (**B**) *Pax5$^{fl/+}$;Rosa26-CreER^{T2}* mice were assigned to five different groups and bred as described in the Chapter 1. The mice at 6 weeks of age were intraperitoneally (i.p.) administered 75 mg/kg tamoxifen (Tam; T5648, Sigma-Aldrich Japan, Tokyo), dissolved in peanut oil (P2144, Sigma-Aldrich Japan), or only peanut oil (Oil) for three consecutive days. One week after the injection of the Tam or Oil, the mice (about 7 weeks of age) in the irradiated groups were exposed to a single whole-body dose of 4 or 2 Gy gamma rays at 0.4 Gy/min using a ^{137}Cs source (Gammacell-40, Nordion). When mice became 60 weeks of age or moribundly, they will be euthanized and autopsied for histopathological analysis of lymphomas (described in the Chapter 1). All experimental procedures were conducted according to the Guidelines for Animal Welfare and Experimentation of NIRS, QST (No. 19-1017). Since this experiment is still in progress, in this thesis, the data until 45 weeks of age are presented as preliminary results.

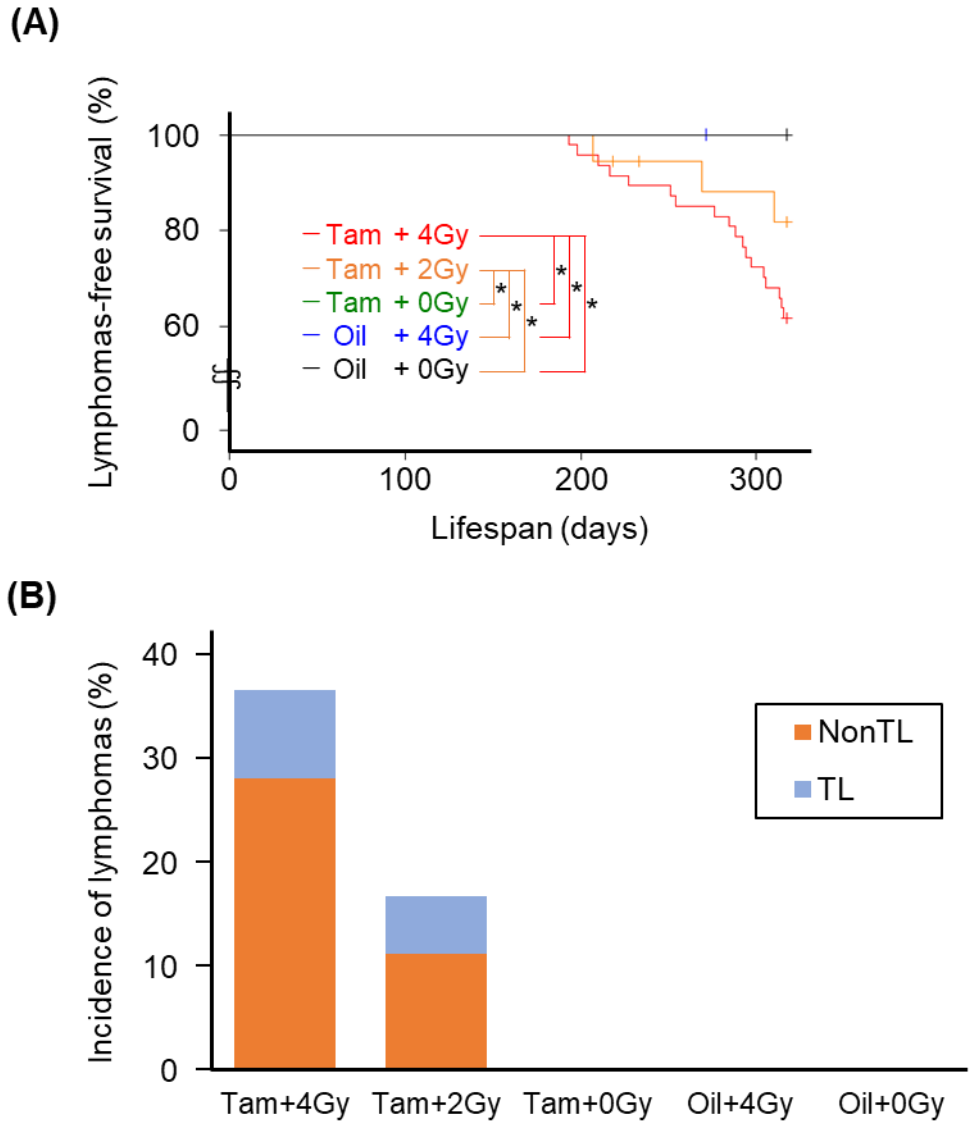

Figure 18. Induction of lymphomas in *Pax5$^{fl/+}$;Rosa26-CreER^{T2}* mice.

(**A**) Overall lymphomas–free survival of the five experimental groups. Kaplan–Meier curves are shown. Asterisks denote significant differences between curves (P<0.05, log-rank test). (**B**) The incidence of thymic lymphoma (TL) and Non-TL, which are generally diagnosed as T-cell and B-cell lymphomas, respectively. Immunophenotype-based classification of the lymphomas and their molecular characteristics will be reported in near future.

GENERAL DISCUSSION

Epidemiological studies of atomic bomb survivors have shown an increased risk of lymphoblastic leukemia/lymphoma, a neoplasm of precursor lymphocyte, after exposure to ionizing radiation [16, 89]. In other studies, a relatively younger age at exposure has been shown to correlate with increased risk for developing acute lymphoblastic leukemia and acute/chronic myeloid leukemias [29, 30]. Lymphoid tumors, including leukemia, are classified according to cells of origin; however, the cell type and the differentiation stage of the leukemic cells are still not clear. About 75 % of human lymphoid tumors are B-cell neoplasms [31]. Therefore, the present study aimed to elucidate the risk of radiation-induced B-cell lymphoma/leukemia according to the cell type and the differentiation stage as well as their underlying mechanisms by using a mouse model.

In the present study, lymphoid neoplasms developed in non-irradiated mice or mice irradiated gamma-rays in infancy or young adulthood were classified into precursor B-cell lymphomas (i.e., pro-B and pre-B types), mature B-cell lymphoma (i.e., mature-B type) and T-cell lymphoma by histopathological and immunophenotype analyses (Chapter 1). Based on this classification, the risk was estimated for each lymphoma-type. These analyses revealed the early induction and the increased risk of precursor B-cell lymphoma in mice irradiated with gamma-rays in infancy or young adulthood compared to non-irradiated control mice [57].

By using approaches based on next-generation sequencing, genetic alterations in the early-onset precursor B-cell lymphomas were further investigated by comparing with the data of late-onset and spontaneously developed B-cell lymphomas (Chapter 2). These analyses showed that chromosomal interstitial deletions including the *Pax5* locus and

gain-of-function mutations of *Jak3* are candidate driver events for the early-onset precursor B-cell lymphomas induced by radiation exposure. Notably, the chromosomal interstitial deletions, including tumor suppressor *Spfi1*, *Ptch1* and *Tsc2* genes, are found as molecular signatures of radiation-induced tumors in several rodent models for acute myeloid leukemia, medulloblastoma and renal cancer, respectively [78, 81, 90]. These observations suggest that the chromosomal interstitial deletion including particular tumor suppressor genes is a radiation-specific mutational event for cancer development following exposure to radiation. Furthermore, the present study revealed that genomic alterations in the early-onset precursor B-cell lymphoma, including the *Pax5* deletion, mutations activating Jak/Stat signaling and lack of oncogenic fusion genes, recapitulate the features of human Philadelphia chromosome (Ph)-like ALL, which is known to be poor outcome after conventional therapeutic approaches [72-76].

Cancer is the result of a complex multistep process that involves the accumulation of several sequential molecular abnormalities and the clonal expansion of mutant cells [1]. The present study identified several key events involved in radiation-induced precursor B-cell lymphomas for the first time. Further *in vivo* studies will clarify the temporal sequence of molecular events and the evolutionary dynamics of cancer cells in radiation-induced B-cell leukemogenesis.

In conclusion, the present study revealed that exposure to ionizing radiation increases the risk of precursor B-cell lymphoma in mice. Chromosomal interstitial deletions including the *Pax5* and *Jak3* mutations were identified as molecular signatures for radiation-induced early-onset precursor B-cell lymphoma. The genomic profile observed in the lymphoma was similar to that found in human Ph-like ALL. The findings obtained in the present study provide new insights into the risk assessment of

lymphoma/leukemia after radiation exposure, molecular mechanisms contributing to radiation carcinogenesis and molecular targeted therapies of radiation-associated B-ALL.

REFERENCES

1 Vogelstein B, Papadopoulos N, Velculescu VE, Zhou S, Diaz LA, Jr., Kinzler KW. Cancer genome landscapes. Science. 2013; 339:1546-1558.

2 Sharma S, Kelly TK, Jones PA. Epigenetics in cancer. Carcinogenesis. 2010; 31:27-36.

3 Mitelman F, Johansson B, Mertens F. The impact of translocations and gene fusions on cancer causation. Nat Rev Cancer. 2007; 7:233-245.

4 Inoue K, Fry EA. Haploinsufficient tumor suppressor genes. Adv Med Biol. 2017; 118:83-122.

5 Fearon ER, Vogelstein B. A genetic model for colorectal tumorigenesis. Cell. 1990; 61:759-767.

6 Walther A, Johnstone E, Swanton C, Midgley R, Tomlinson I, Kerr D. Genetic prognostic and predictive markers in colorectal cancer. Nat Rev Cancer. 2009; 9:489-499.

7 Bhargavan M. Trends in the utilization of medical procedures that use ionizing radiation. Health Phys. 2008; 95:612-627.

8 Mettler FA, Jr., Thomadsen BR, Bhargavan M, Gilley DB, Gray JE, Lipoti JA et al. Medical radiation exposure in the U.S. in 2006: preliminary results. Health Phys. 2008; 95:502-507.

9 Barcellos-Hoff MH, Park C, Wright EG. Radiation and the microenvironment - tumorigenesis and therapy. Nat Rev Cancer. 2005; 5:867-875.

10 McGlynn SP, Rupnik K, Varma MN, Klasinc L. Radiation Signatures and Radiation Markers. Radiation Protection Dosimetry. 1994; 52:155-164.

11 Nakano T, Xu X, Salem AMH, Shoulkamy MI, Ide H. Radiation-induced DNA-protein cross-links: Mechanisms and biological significance. Free Radic Biol Med. 2017; 107:136-145.

12 Prise KM, Pinto M, Newman HC, Michael BD. A review of studies of ionizing radiation-induced double-strand break clustering. Radiat Res. 2001; 156:572-576.

13 Mao Z, Bozzella M, Seluanov A, Gorbunova V. DNA repair by nonhomologous end joining and homologous recombination during cell cycle in human cells. Cell Cycle. 2008; 7:2902-2906.

14 Rothkamm K, Kühne M, Jeggo PA, Löbrich M. Radiation-induced genomic rearrangements formed by nonhomologous end-joining of DNA double-strand breaks. Cancer Res. 2001; 61:3886-3893.

15 Morgan WF, Corcoran J, Hartmann A, Kaplan MI, Limoli CL, Ponnaiya B. DNA double-strand breaks, chromosomal rearrangements, and genomic instability. Mutat Res. 1998; 404:125-128.

16 Hsu WL, Preston DL, Soda M, Sugiyama H, Funamoto S, Kodama K et al. The incidence of leukemia, lymphoma and multiple myeloma among atomic bomb survivors: 1950-2001. Radiat Res. 2013; 179:361-382.

17 Preston DL, Ron E, Tokuoka S, Funamoto S, Nishi N, Soda M et al. Solid cancer incidence in atomic bomb survivors: 1958-1998. Radiat Res. 2007; 168:1-64.

18 Inaba H, Greaves M, Mullighan CG. Acute lymphoblastic leukaemia. Lancet. 2013; 381:1943-1955.

19 Olsen Saraiva Camara N, Lepique AP, Basso AS. Lymphocyte differentiation and effector functions. Clin Dev Immunol. 2012; 2012:510603.

20 Cobaleda C, Schebesta A, Delogu A, Busslinger M. Pax5: the guardian of B cell identity and function. Nat Immunol. 2007; 8:463-470.

21 Blyth BJ, Kakinuma S, Sunaoshi M, Amasaki Y, Hirano-Sakairi S, Ogawa K et al. Genetic Analysis of T Cell Lymphomas in Carbon Ion-Irradiated Mice Reveals Frequent Interstitial Chromosome Deletions: Implications for Second Cancer Induction in Normal Tissues during Carbon Ion Radiotherapy. PLoS One. 2015; 10:e0130666.

22 Shang Y, Kakinuma S, Yamauchi K, Morioka T, Kokubo T, Tani S et al. Cancer prevention by adult-onset calorie restriction after infant exposure to ionizing radiation in B6C3F1 male mice. Int J Cancer. 2014; 135:1038-1047.

23 Grant EJ, Brenner A, Sugiyama H, Sakata R, Sadakane A, Utada M et al. Solid Cancer Incidence among the Life Span Study of Atomic Bomb Survivors: 1958-2009. Radiat Res. 2017; 187:513-537.

24 Richardson D, Sugiyama H, Nishi N, Sakata R, Shimizu Y, Grant EJ et al. Ionizing radiation and leukemia mortality among Japanese Atomic Bomb Survivors, 1950-2000. Radiat Res. 2009; 172:368-382.

25 Meadows AT, Friedman DL, Neglia JP, Mertens AC, Donaldson SS, Stovall M et al. Second neoplasms in survivors of childhood cancer: findings from the Childhood Cancer Survivor Study cohort. J Clin Oncol. 2009; 27:2356-2362.

26 Kumar S. Second malignant neoplasms following radiotherapy. Int J Environ Res Public Health. 2012; 9:4744-4759.

27 Brody AS, Frush DP, Huda W, Brent RL. Radiation risk to children from computed tomography. Pediatrics. 2007; 120:677-682.

28 UNSCEAR. Effects of radiation exposure of children, vol. II. UNITED NATIONS

PUBLICATION, 2013.

29 Friedman DL, Whitton J, Leisenring W, Mertens AC, Hammond S, Stovall M et al. Subsequent neoplasms in 5-year survivors of childhood cancer: the Childhood Cancer Survivor Study. J Natl Cancer Inst. 2010; 102:1083-1095.

30 Shivakumar R, Tan W, Wilding GE, Wang ES, Wetzler M. Biologic features and treatment outcome of secondary acute lymphoblastic leukemia--a review of 101 cases. Ann Oncol. 2008; 19:1634-1638.

31 Morton LM, Wang SS, Devesa SS, Hartge P, Weisenburger DD, Linet MS. Lymphoma incidence patterns by WHO subtype in the United States, 1992-2001. Blood. 2006; 107:265-276.

32 Morioka T, Blyth BJ, Imaoka T, Nishimura M, Takeshita H, Shimomura T et al. Establishing the Japan-Store house of animal radiobiology experiments (J-SHARE), a large-scale necropsy and histopathology archive providing international access to important radiobiology data. Int J Radiat Biol. 2019:1-6.

33 Rehg JE, Bush D, Ward JM. The utility of immunohistochemistry for the identification of hematopoietic and lymphoid cells in normal tissues and interpretation of proliferative and inflammatory lesions of mice and rats. Toxicol Pathol. 2012; 40:345-374.

34 Morioka T, Miyoshi-Imamura T, Blyth BJ, Kaminishi M, Kokubo T, Nishimura M et al. Ionizing radiation, inflammation, and their interactions in colon carcinogenesis in Mlh1-deficient mice. Cancer Sci. 2015; 106:217-226.

35 Mikkola HK, Orkin SH. The journey of developing hematopoietic stem cells. Development. 2006; 133:3733-3744.

36 Cohen Hubal EA, de Wet T, Du Toit L, Firestone MP, Ruchirawat M, van Engelen J et al. Identifying important life stages for monitoring and assessing risks from exposures to environmental contaminants: results of a World Health Organization review. Regul Toxicol Pharmacol. 2014; 69:113-124.

37 Ward JM. Lymphomas and leukemias in mice. Exp Toxicol Pathol. 2006; 57:377-381.

38 Cheng Y, Chikwava K, Wu C, Zhang H, Bhagat A, Pei D et al. LNK/SH2B3 regulates IL-7 receptor signaling in normal and malignant B-progenitors. J Clin Invest. 2016; 126:1267-1281.

39 Daino K, Ishikawa A, Suga T, Amasaki Y, Kodama Y, Shang Y et al. Mutational landscape of T-cell lymphoma in mice lacking the DNA mismatch repair gene Mlh1: no synergism with ionizing radiation. Carcinogenesis. 2019; 40:216-224.

40 van der Weyden L, Giotopoulos G, Rust AG, Matheson LS, van Delft FW, Kong

J et al. Modeling the evolution of ETV6-RUNX1-induced B-cell precursor acute lymphoblastic leukemia in mice. Blood. 2011; 118:1041-1051.

41 Ishizawa S, Slovak ML, Popplewell L, Bedell V, Wrede JE, Carter NH et al. High frequency of pro-B acute lymphoblastic leukemia in adults with secondary leukemia with 11q23 abnormalities. Leukemia. 2003; 17:1091-1095.

42 Shu XO, Potter JD, Linet MS, Severson RK, Han D, Kersey JH et al. Diagnostic X-rays and ultrasound exposure and risk of childhood acute lymphoblastic leukemia by immunophenotype. Cancer Epidemiol Biomarkers Prev. 2002; 11:177-185.

43 Decleve A, Gerber GB, Leonard A, Lambiet-Collier M, Sassen A, Maisin JR. Regneration of thymus, spleen and bone marrow in x-irradiated AKR mice. Radiat Res. 1972; 51:318-332.

44 Sado T, Kamisaku H, Kubo E. Bone marrow-thymus interactions during thymic lymphomagenesis induced by fractionated radiation exposure in B10 mice: analysis using bone marrow transplantation between Thy 1 congenic mice. J Radiat Res. 1991; 32 Suppl 2:168-180.

45 Utsuyama M, Hirokawa K. Radiation-induced-thymic lymphoma occurs in young, but not in old mice. Exp Mol Pathol. 2003; 74:319-325.

46 Arslan C, Ozdemir E, Dogan E, Ozisik Y, Altundag K. Secondary hematological malignancies after treatment of non-metastatic breast cancer. J buon. 2011; 16:744-750.

47 Verbiest T, Finnon R, Brown N, Cruz-Garcia L, Finnon P, O'Brien G et al. Tracking preleukemic cells in vivo to reveal the sequence of molecular events in radiation leukemogenesis. Leukemia. 2018; 32:1435-1444.

48 Nakamura N. A hypothesis: radiation-related leukemia is mainly attributable to the small number of people who carry pre-existing clonally expanded preleukemic cells. Radiat Res. 2005; 163:258-265.

49 Portell CA, Wenzell CM, Advani AS. Clinical and pharmacologic aspects of blinatumomab in the treatment of B-cell acute lymphoblastic leukemia. Clin Pharmacol. 2013; 5:5-11.

50 Roberts KG, Mullighan CG. The Biology of B-Progenitor Acute Lymphoblastic Leukemia. Cold Spring Harb Perspect Med. 2020; 10.

51 Koboldt DC, Zhang Q, Larson DE, Shen D, McLellan MD, Lin L et al. VarScan 2: somatic mutation and copy number alteration discovery in cancer by exome sequencing. Genome Res. 2012; 22:568-576.

52 Cingolani P, Platts A, Wang le L, Coon M, Nguyen T, Wang L et al. A program for annotating and predicting the effects of single nucleotide polymorphisms, SnpEff: SNPs in the genome of Drosophila melanogaster strain w1118; iso-2; iso-3. Fly (Austin). 2012; 6:80-92.

53 Boeva V, Popova T, Bleakley K, Chiche P, Cappo J, Schleiermacher G et al. Control-FREEC: a tool for assessing copy number and allelic content using next-generation sequencing data. Bioinformatics. 2012; 28:423-425.

54 Subramanian A, Tamayo P, Mootha VK, Mukherjee S, Ebert BL, Gillette MA et al. Gene set enrichment analysis: a knowledge-based approach for interpreting genome-wide expression profiles. Proc Natl Acad Sci U S A. 2005; 102:15545-15550.

55 Haas BJ, Dobin A, Stransky N, Li B, Yang X, Tickle T et al. STAR-Fusion: Fast and Accurate Fusion Transcript Detection from RNA-Seq. bioRxiv. 2017:120295.

56 Wang J, Valdez A, Chen Y. Evaluation of automated Wes system as an analytical and characterization tool to support monoclonal antibody drug product development. J Pharm Biomed Anal. 2017; 139:263-268.

57 Tachibana H, Morioka T, Daino K, Shang Y, Ogawa M, Fujita M et al. Early induction and increased risk of precursor B-cell neoplasms after exposure of infant or young-adult mice to ionizing radiation. J Radiat Res. 2020; 61:648-656.

58 Sondka Z, Bamford S, Cole CG, Ward SA, Dunham I, Forbes SA. The COSMIC Cancer Gene Census: describing genetic dysfunction across all human cancers. Nat Rev Cancer. 2018; 18:696-705.

59 Martin-Lorenzo A, Hauer J, Vicente-Duenas C, Auer F, Gonzalez-Herrero I, Garcia-Ramirez I et al. Infection Exposure is a Causal Factor in B-cell Precursor Acute Lymphoblastic Leukemia as a Result of Pax5-Inherited Susceptibility. Cancer Discov. 2015; 5:1328-1343.

60 Batista CR, Lim M, Laramée AS, Abu-Sardanah F, Xu LS, Hossain R et al. Driver mutations in Janus kinases in a mouse model of B-cell leukemia induced by deletion of PU.1 and Spi-B. Blood Adv. 2018; 2:2798-2810.

61 Flex E, Petrangeli V, Stella L, Chiaretti S, Hornakova T, Knoops L et al. Somatically acquired JAK1 mutations in adult acute lymphoblastic leukemia. J Exp Med. 2008; 205:751-758.

62 Sic H, Speletas M, Cornacchione V, Seidl M, Beibel M, Linghu B et al. An Activating Janus Kinase-3 Mutation Is Associated with Cytotoxic T Lymphocyte Antigen-4-Dependent Immune Dysregulation Syndrome. Front Immunol. 2017; 8:1824.

63 Degryse S, de Bock CE, Cox L, Demeyer S, Gielen O, Mentens N et al. JAK3 mutants transform hematopoietic cells through JAK1 activation, causing T-cell acute lymphoblastic leukemia in a mouse model. Blood. 2014; 124:3092-3100.

64 Fazio G, Cazzaniga V, Palmi C, Galbiati M, Giordan M, te Kronnie G et al. PAX5/ETV6 alters the gene expression profile of precursor B cells with opposite dominant effect on endogenous PAX5. Leukemia. 2013; 27:992-995.

65 Mullighan CG, Goorha S, Radtke I, Miller CB, Coustan-Smith E, Dalton JD et al. Genome-wide analysis of genetic alterations in acute lymphoblastic leukaemia. Nature. 2007; 446:758-764.

66 Mori S, Rempel RE, Chang JT, Yao G, Lagoo AS, Potti A et al. Utilization of pathway signatures to reveal distinct types of B lymphoma in the Emicro-myc model and human diffuse large B-cell lymphoma. Cancer Res. 2008; 68:8525-8534.

67 Clark MR, Mandal M, Ochiai K, Singh H. Orchestrating B cell lymphopoiesis through interplay of IL-7 receptor and pre-B cell receptor signalling. Nat Rev Immunol. 2014; 14:69-80.

68 Sun B, Mallampati S, Gong Y, Wang D, Lefebvre V, Sun X. Sox4 is required for the survival of pro-B cells. J Immunol. 2013; 190:2080-2089.

69 Winkler TH, Mårtensson IL. The Role of the Pre-B Cell Receptor in B Cell Development, Repertoire Selection, and Tolerance. Front Immunol. 2018; 9:2423.

70 Familiades J, Bousquet M, Lafage-Pochitaloff M, Béné MC, Beldjord K, De Vos J et al. PAX5 mutations occur frequently in adult B-cell progenitor acute lymphoblastic leukemia and PAX5 haploinsufficiency is associated with BCR-ABL1 and TCF3-PBX1 fusion genes: a GRAALL study. Leukemia. 2009; 23:1989-1998.

71 Ramos HL, O'Shea JJ, Watford WT. STAT5 isoforms: controversies and clarifications. Biochem J. 2007; 404:e1-2.

72 Mullighan CG, Zhang J, Harvey RC, Collins-Underwood JR, Schulman BA, Phillips LA et al. JAK mutations in high-risk childhood acute lymphoblastic leukemia. Proc Natl Acad Sci U S A. 2009; 106:9414-9418.

73 Pui CH, Roberts KG, Yang JJ, Mullighan CG. Philadelphia Chromosome-like Acute Lymphoblastic Leukemia. Clin Lymphoma Myeloma Leuk. 2017; 17:464-470.

74 Roberts KG, Li Y, Payne-Turner D, Harvey RC, Yang YL, Pei D et al. Targetable kinase-activating lesions in Ph-like acute lymphoblastic leukemia. N Engl J Med. 2014; 371:1005-1015.

75 Harvey RC, Mullighan CG, Wang X, Dobbin KK, Davidson GS, Bedrick EJ et al. Identification of novel cluster groups in pediatric high-risk B-precursor acute lymphoblastic leukemia with gene expression profiling: correlation with genome-wide DNA copy number alterations, clinical characteristics, and outcome. Blood. 2010; 116:4874-4884.

76 Frisch A, Ofran Y. How I diagnose and manage Philadelphia chromosome-like acute lymphoblastic leukemia. Haematologica. 2019; 104:2135-2143.

77 Cao Y, Zhu T, Zhang P, Xiao M, Yi S, Yang Y et al. Mutations or copy number losses of CD58 and TP53 genes in diffuse large B cell lymphoma are independent unfavorable prognostic factors. Oncotarget. 2016; 7:83294-83307.

78 Silver A, Moody J, Dunford R, Clark D, Ganz S, Bulman R et al. Molecular mapping of chromosome 2 deletions in murine radiation-induced AML localizes a putative tumor suppressor gene to a 1.0 cM region homologous to human chromosome segment 11p11-12. Genes Chromosomes Cancer. 1999; 24:95-104.

79 Pazzaglia S, Mancuso M, Atkinson MJ, Tanori M, Rebessi S, Majo VD et al. High incidence of medulloblastoma following X-ray-irradiation of newborn Ptc1 heterozygous mice. Oncogene. 2002; 21:7580-7584.

80 Ishida Y, Takabatake T, Kakinuma S, Doi K, Yamauchi K, Kaminishi M et al. Genomic and gene expression signatures of radiation in medulloblastomas after low-dose irradiation in Ptch1 heterozygous mice. Carcinogenesis. 2010; 31:1694-1701.

81 Inoue T, Kokubo T, Daino K, Yanagihara H, Watanabe F, Tsuruoka C et al. Interstitial chromosomal deletion of the tuberous sclerosis complex 2 locus is a signature for radiation-associated renal tumors in Eker rats. Cancer Sci. 2020; 111:840-848.

82 Hirokawa S, Sato H, Kato I, Kudo A. EBF-regulating Pax5 transcription is enhanced by STAT5 in the early stage of B cells. Eur J Immunol. 2003; 33:1824-1829.

83 Firtina S, Sayitoglu M, Hatirnaz O, Erbilgin Y, Oztunc C, Cinar S et al. Evaluation of PAX5 gene in the early stages of leukemic B cells in the childhood B cell acute lymphoblastic leukemia. Leuk Res. 2012; 36:87-92.

84 Dang J, Wei L, de Ridder J, Su X, Rust AG, Roberts KG et al. PAX5 is a tumor suppressor in mouse mutagenesis models of acute lymphoblastic leukemia. Blood. 2015; 125:3609-3617.

85 Gery S, Koeffler HP. Role of the adaptor protein LNK in normal and malignant hematopoiesis. Oncogene. 2013; 32:3111-3118.

86 Nik-Zainal S, Alexandrov LB, Wedge DC, Van Loo P, Greenman CD, Raine K et al. Mutational processes molding the genomes of 21 breast cancers. Cell. 2012; 149:979-993.

87 Horcher M, Souabni A, Busslinger M. Pax5/BSAP maintains the identity of B cells in late B lymphopoiesis. Immunity. 2001; 14:779-790.

88 Ventura A, Kirsch DG, McLaughlin ME, Tuveson DA, Grimm J, Lintault L et al. Restoration of p53 function leads to tumour regression in vivo. Nature. 2007; 445:661-665.

89 Fujihara M, Sakata R, Yoshida N, Ozasa K, Preston DL, Mabuchi K. Incidence of lymphoid neoplasms among atomic bomb survivors by histological subtype: 1950-1994. Blood. 2021.

90 Tsuruoka C, Blyth BJ, Morioka T, Kaminishi M, Shinagawa M, Shimada Y et al. Sensitive Detection of Radiation-Induced Medulloblastomas after Acute or Protracted Gamma-Ray Exposures in Ptch1 Heterozygous Mice Using a Radiation-Specific Molecular Signature. Radiat Res. 2016; 186:407-414.

ACKNOWLEDGEMENTS

I would like to thank Prof. Akira Matsuura, Prof. Eisuke Itakura, Dr. Shizuko Kakinuma, Dr. Kazuhiro Daino, Dr. Takamitsu Morioka, Dr. Tatsuhiko Imaoka, Dr. Daisuke Iizuka, Dr. Yi Shang, Dr. Chizuru Tsuruoka, Dr. Masaaki Sunaoshi and Dr. Yoshiya Shimada for their suggestion and discussions throughout my thesis. I am grateful to all member of Laboratory of Molecular and Cellular Biology laboratory in Chiba University and Department of Radiation Effects Research in National Institutes for Quantum Science and Technology. The present study was supported in part by Grant-in-Aid for JSPS Fellows (JP21J0496).